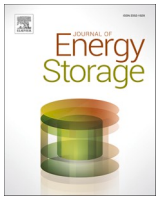
Journal of Energy Storage 182 (2026) 124913



Contents lists available at ScienceDirect

Journal of Energy Storage

journal homepage: www.elsevier.com/locate/est



Research Papers

Techno-economic assessment of converting a coal-fired power plant into a renewable solar power plant with thermal energy storage

Javier Iñigo-Labairu [a,*], Stefano Giuliano [b], Robert Pitz-Paal [a]

[a] German Aerospace Center (DLR), Institute of Solar Research, Linder Höhe, 51147, Köln, Germany
[b] German Aerospace Center (DLR), Institute of Solar Research, Pfaffenwaldring 38-40, 70569, Stuttgart, Germany

ARTICLE INFO

Keywords:
Hybrid solar energy system
Concentrating solar power
Thermal energy storage
Carnot battery
Techno-economic analysis
Coal plant retrofitting

ABSTRACT

This study evaluates the conversion of the Angamos coal-fired power plant in Chile into a renewable power plant through a techno-economic comparison of different energy configurations integrating solar generation and energy storage. The analyzed configurations include: a hybrid PV-parabolic trough plant with thermal energy storage (TES), a hybrid PV-solar tower plant with TES, a standalone CSP tower plant with TES, a PV plant with battery storage, and a Carnot battery coupled with PV, an electric heater, and TES. The operational strategy is a key factor in the assessment of these plants. Two main options were considered: baseload operation, aiming for continuous 24/7 production, and a storage-based strategy, in which electricity is only produced at night to compensate for the lack of renewable generation during these hours. The latter strategy was analyzed both with an on-site PV plant and with a hypothetical, grid connected PV plant assumed to supply any required amount of electricity at a fixed price. Scenarios of "Brownfield" (reusing the existing power block) and "Greenfield" (new build) were assessed. The results of the techno-economic analysis indicate that hybrid CSP-PV plants achieve costs similar to Carnot batteries and lower than conventional batteries for high nighttime capacity factors. Operating strategy and cost assumptions are decisive for the competitiveness of each alternative.

1. Introduction

The decarbonization of the power sector requires not only the large-scale deployment of renewable energy technologies but also the availability of flexible resources that ensure security of supply and carbon-free electricity generation during periods of low solar availability. Electricity generation from photovoltaic (PV) systems has experienced a significant cost reduction over the past decade [1], enabling a substantial increase in the renewable share and becoming the lowest-cost electricity generation technology in many regions. However, PV generation remains dependent on a variable solar resource and provides limited inertia to the power grid. Therefore, measures aimed at improving system reliability and integrating energy storage are necessary to achieve a fully renewable power system.

Energy storage is thus a key element in the complete decarbonization of the electricity system. Battery Energy Storage Systems (BESS) represent a promising option, as their costs have declined significantly in recent years [1–3], and they constitute a mature technology with high efficiencies and fast response times. Nevertheless, storage costs remain high for large energy capacities, posing a challenge for covering total electricity demand. In contrast, Thermal Energy Storage (TES) is a cost-effective technology for long-duration storage and has already been demonstrated at high temperatures in Concentrated Solar Power (CSP) plants using molten salts [4].

In parallel with the continued expansion of renewable energy deployment, a substantial global fleet of coal-fired power plants remains in operation. Many of these plants still have significant remaining lifetimes and support a large number of jobs, while also contributing large volumes of CO_2 emissions. According to the International Energy Agency [5,6], if the current worldwide coal fleet were operated over typical lifetimes, it would emit roughly 330 Gt of CO_2, posing a major barrier to meeting climate targets. This fleet comprises about 9000 coal power plants with around 2185 GW of capacity, most of which are located in emerging and developing economies. In 2022 alone, emissions from coal-fired generation reached an all-time high of approximately 15.5 Gt of CO_2. Data from GEM [7] show that total coal capacity has increased by over 13% since the 2015 Paris Climate Agreement. In 2024, capacity additions continued to outpace retirements, largely due to new plants in China and India. Retirements, however, have accelerated in some regions. For example, all but three EU countries plan to

* Corresponding author.
E-mail addresses: javier.inigolabairu@dlr.de (J. Iñigo-Labairu), stefano.giuliano@dlr.de (S. Giuliano), robert.pitz-paal@dlr.de (R. Pitz-Paal).

https://doi.org/10.1016/j.est.2026.124913
Received 23 April 2026; Received in revised form 20 August 2026; Accepted 26 September 2026
2352-152X/© 2026 The Authors. Published by Elsevier Ltd. This is an open access article under the CC BY license (http://creativecommons.org/licenses/by/4.0/).
Open access funding enabled and organized by Projekt DEAL.

phase out coal by 2033, and retirements in the region quadrupled from 2.7 GW in 2023 to 11 GW in 2024. According to the Global Coal Plant Tracker [8,9], coal-fired units have typically been retired after about 38 years of operation, although the average age varies widely by region. Looking forward, the Tracker indicates that around 1780 GW of existing coal capacity could still be operating in 2035, consisting of units without a defined retirement date or national phaseout commitment. Of this capacity, the average plant would have been in operation for 29 years by 2035, and 44 years outside of China.

Within this context, converting existing coal-fired power plants into renewable energy facilities represents an attractive option to contribute to power sector decarbonization, generate positive economic impacts, and enable the reuse of valuable infrastructure. The reutilization of components such as the power block or the grid connection can significantly reduce investment costs and accelerate renewable deployment. Such retrofitting of coal plants can be combined with CSP plants in regions with suitable solar resources and land availability, or alternatively implemented in the form of Carnot batteries using power-to-heat components.

At the same time, the drastic reduction in PV generation costs has made CSP technology less competitive in terms of daytime electricity production. However, the high costs associated with large-scale electrical energy storage make the technological hybridization of CSP and PV plants attractive, as it leverages the advantages of both technologies. On one hand, low-cost PV electricity generated during daytime hours can be used to supply cheap electricity while simultaneously charging thermal energy storage via power-to-heat technologies. On the other hand, stored energy from the CSP field or the power-to-heat unit can be discharged during nighttime, taking advantage of the lower costs of thermal storage and using the power block for electricity generation.

In recent years, a significant number of studies have analyzed hybrid CSP-PV systems. The advantages of CSP hybridization have been summarized in several reviews, highlighting the increased dispatchability and reliability of integrated CSP-PV systems [10], the technological complementarity between PV and CSP which improves power quality and efficiency [11], as well as comparisons with other hybridization approaches, emphasizing the role of thermal energy storage in ensuring continuous supply and reducing costs by sharing major equipment [12]. Comprehensive integration of CSP and PV plants has also been analyzed in previous techno-economic studies [13,14], exploiting component synergies and coupling with power-to-heat units across different locations. Comparisons with other technologies show levelized cost of electricity (LCOE) values similar to those of Carnot battery systems, lower than PV BESS combinations for storage capacities above approximately four hours, and a strong sensitivity of results to assumed costs.

Guccione et al. [15] explored the integration of supercritical CO_2 (sCO_2) power cycles into CSP plants and their hybridization with PV systems through electric heaters (EH), showing significant techno-economic advantages. Results indicate that hybrid CSP-PV configurations, particularly when combined with sCO_2 power blocks, can reduce the levelized cost of electricity by up to 42% at small scales and offer cost-effective solutions for capacity factors (CF) above 60%, while PV BESS or PV-EH hybrids are more suitable for lower capacity factors. The Chilean case has been frequently studied due to its high solar irradiance. Parrado et al. [16] analyzed a hybrid PV–CSP plant in the Atacama Desert, showing that combining a 20 MW_p PV field with a 30 MW CSP plant equipped with 15 h of thermal energy storage can provide continuous electricity, reduce the LCOE, and meet the electricity demand of the mining industry in the region. Moreover, this configuration can contribute to price stabilization and CO_2 emission reduction in Chile. The Atacama Desert has also been analyzed with hybrid CSP-PV configurations by Starke et al. [17], again highlighting the potential of the technological combination. Zurita et al. [18] presented a techno-economic analysis of a hybrid plant combining a solar tower (ST), PV arrays, TES, and BESS. Component sizes were varied to identify configurations with the lowest LCOE and to determine the capacity factor. Results showed that significant reductions in BESS costs are necessary for hybrid systems including batteries to remain competitive. The configuration with the lowest LCOE was a CSP-PV plant with tracked PV arrays.

Behar et al. [19] analyzed the most competitive solar technology for integration into existing copper mining plants, finding that PV plants had the lowest costs, approximately four times lower than CSP plants and 50% lower than hybrid plants. While hybridization presents opportunities, reductions in CSP component costs are still necessary. In this analysis, energy storage for PV or hybrid plants was not considered, with the grid used to cover unmet demand. Other locations and countries have also been analyzed in techno-economic studies, demonstrating the impact of solar resources and assumed costs on results. A comparison between CSP-PV systems with thermal energy storage and PV BESS configurations was presented by Aguilar-Jiménez et al. [20] for an isolated microgrid in Baja California. The CSP-PV system presented an LCOE only 2% higher than the PV BESS system, but this value decreased if the organic Rankine cycle (ORC) capacity was increased to 60 kW_{el}. Additionally, larger community demand or energy maximization contributed to further reductions in the calculated LCOE.

System design and optimization is another key aspect of hybrid systems. Pilotti et al. [21] developed a mixed-integer linear programming model for the simultaneous design and operational optimization of highly integrated CSP-PV plants, including the use of electric heaters to convert excess PV electricity into heat stored in the CSP thermal storage. Their results demonstrated that hybrid CSP-PV configurations can achieve similar or higher dispatchability levels than standalone CSP or PV BESS systems while reducing the LCOE by approximately 30–50% through improved integration and energy sharing. Furlan et al. [22] applied a robust multi-objective optimization framework to assess the techno-economic and environmental performance of hybrid CSP-PV plants under uncertainty. Results for Ivanpah, California indicate that hybridization can reduce LCOE by around 41% compared to standalone CSP, while revealing key design trade-offs between PV reliance, solar concentrator area, and backup boiler use. Operational strategy is also a critical factor, affecting both economic outcomes and plant design. Zurita et al. [23] analyzed, using a multi-objective optimization approach, how different dispatch strategies (baseload, daylight, night, and daylight-and-evening) impact the optimal design and competitiveness of PV, CSP, and hybrid CSP-PV plants with storage, showing that system configuration and LCOE strongly depend on the selected strategy and location.

Another renewable option for nighttime electricity production that ensures dispatchability and reliability is the Carnot battery. In this configuration, thermal energy storage is charged through a power-to-heat (P2H) unit and subsequently discharged to produce electricity using a power block (PB). In this way, the power-to-heat unit can also be supplied by a PV field. This option is particularly suitable for the reuse of power blocks from coal-fired power plants worldwide [24].

Various forms of Carnot batteries have been extensively described in several reviews [25–29], including their level of technological development, commercial plants, and the main technical challenges they face. These studies demonstrate the potential of the technology for large-scale applications and its ability to provide dispatchable energy through different technological configurations, considering various thermodynamic cycles such as Rankine or supercritical CO_2, and the integration of thermal storage with different media such as molten salt, solid media, or liquid air. The literature highlights the capacity of Carnot batteries to enhance grid flexibility, increase renewable energy penetration, and decarbonize coal-fired plants. Key challenges include efficiency losses, system scalability, and high costs compared to other storage technologies. The specific application of Carnot batteries for the decarbonization of coal-fired power plants has been addressed in several studies. Arnold et al. [30] demonstrated the technical feasibility of integrating high-temperature thermal energy storage into existing coal-fired power plants using molten salt and solid/air storage technologies, including

Carnot battery configurations. The study concluded that thermal storage power plants (TSPP) can represent a short-term, large-scale option that makes extensive use of existing infrastructure, enabling a socially sustainable expansion of renewable energy as both baseload and dispatchable generation, and thereby making a significant contribution to future CO_2-free electricity and heat production. Roldán et al. [31] evaluated the retrofit of a Chilean coal-fired power plant with rock-bed thermal energy storage, showing that an 8-h, 5.27 GWh_{th} system can achieve a round-trip efficiency of 34.9% and a minimum LCOE of 88.1 €/MWh_{el}, highlighting the economic viability of thermal storage power plants. The electricity price for charging was identified as a key factor for successful implementation. Geyer et al. [32] analyzed the conversion of a 250 MW_{el} coal-fired power plant in Chile. The simulation of a Carnot battery yielded a round-trip efficiency of approximately 38% and an LCOE below 90 \$/MWh_{el} for 12–14 h of storage. The conversion would enable complete decarbonization of existing coal plants while preserving most on-site employment.

Truong and Bollinger [33] studied the techno-economic potential of converting retiring coal-fired power plants into long-duration energy storage facilities by integrating Malta Pumped Heat Energy Storage (PHES) technology with the existing steam turbines. The analysis shows that this type of repowering can make use of existing infrastructure to support the clean energy transition, preserve local jobs, and be more cost-effective under ambitious carbon-reduction scenarios than equivalent battery systems for storage durations longer than 4 h, with the best repurposing option depending on the plant's age and local requirements. Enervis [34] assessed replacement options for Greece's Ptolemaida V lignite plant, comparing carbon capture and storage, biomass, fossil gas, and TES combined with renewables. The results indicate that TES coupled with renewables is the only fully emission-free option capable of achieving cost parity with fossil gas and biomass retrofits under ambitious CO_2 price scenarios. Zhang et al. [35] developed a co-planning framework combining Carnot battery retrofits with battery storage and variable renewable energy for the Shanxi power system in China. They evaluated economic aspects, implementation pathways, and emission reductions, providing decision-making support for government and system planners. Complementarily, Zhang et al. [36] proposed a multipath retrofit planning approach for coal-fired power plants in low-carbon power system transitions in the same region, identifying optimal conversion strategies. Li et al. [37] explored the conversion of decommissioned coal-fired power plants into Carnot battery systems based on a high-temperature heat pump, molten-salt thermal energy storage, and the existing steam turbine. Their results show that argon as the working fluid enables the highest round-trip efficiency (≈60%) while achieving competitive storage costs, highlighting the techno-economic viability of this approach for large-scale energy storage, with a payback period of 6.39 years. Klasing et al. [38] demonstrated that repurposing supercritical coal-fired power plants with a 620 °C nitrate molten-salt thermal energy storage system enables cost-effective long-duration energy storage (10-h discharge) at lower costs than grid-scale batteries, while reusing existing infrastructure.

Despite the growing relevance of these concepts, a systematic techno-economic comparison of hybrid CSP-PV systems, Carnot batteries, standalone CSP plants, and PV BESS configurations under different operating strategies has scarcely been investigated, particularly in the context of coal-plant conversion. Moreover, the impact of operating strategies, such as baseload operation versus storage-based nighttime dispatch, on system performance and costs is often overlooked, even though it strongly influences optimal plant design and competitiveness. This study addresses these gaps by performing a detailed techno-economic assessment of converting the Angamos coal-fired power plant in northern Chile into various renewable energy configurations based on solar generation and energy storage. Five system concepts are analyzed: hybrid PV–parabolic trough plants with TES, hybrid PV–solar tower plants with TES, a standalone CSP tower plant, a PV plant with battery storage, and a Carnot battery system based on PV, electric heaters, and TES. Each concept is evaluated under different operating strategies and for both brownfield and greenfield scenarios. The analysis focuses on the levelized cost of electricity as well as on indicators that capture nighttime electricity production, thereby providing insights into the trade-offs between cost, dispatchability, and system design in the transition from coal-based to renewable power generation.

2. Concepts and operating strategies

Five energy configurations based on solar power generation and equipped with energy storage were compared. Three operational strategies were considered for each concept, reflecting varying production requirements and boundary conditions, as described in Section 2.1. The technical details of the five energy configurations are then presented in Section 2.2.

2.1. Operating strategies

The operation strategy plays a decisive role in the techno-economic performance of the analyzed power plant concepts. In this study, three different operating strategies were defined, which serve as a common framework for all configurations:

- **Baseload operation with real PV (Baseload):** The load profile of this operating strategy is defined as a continuous 24/7 electricity demand. However, the extent to which this demand can actually be supplied depends on the specific plant configuration and sizing, as well as on the availability of stored energy. During daytime, the PV plant feeds electricity into the grid and simultaneously supplies the auxiliary consumption of the power plant, the electricity demand of the electric heater, or the charging of the battery storage system, if present. The priority order for PV electricity use depends on the specific system configuration. The heat produced by the CSP field is used to charge the thermal energy storage. During nighttime, electricity generation continues either by discharging the TES through the power block or by discharging the BESS. This operating strategy corresponds to what is typically referred to as a "solar-only baseload" supply.
- **Storage-based operation with real PV, nighttime discharge (Night-Real):** In this strategy, electricity is only produced at night. During daytime, the PV plant is fully dedicated to covering the plant's auxiliary consumption and charging the storage system, either directly charging the BESS or indirectly charging the TES through electric heaters. The PB is only dispatched during nighttime hours, as long as sufficient energy is stored. To enable this operation, the PV field is dimensioned to provide the required charging capacity. However, excess electricity that cannot be used for charging cannot be fed into the grid and is therefore curtailed. This strategy focuses on maximizing dispatchable nighttime electricity production.
- **Storage-based operation with fictional PV, nighttime discharge (Night-Fict):** To allow a simplified benchmarking of the different systems, a third operating strategy assumes a hypothetical PV plant with constant daytime generation, from which only the electricity required by the analyzed power plant is taken. In contrast to the second strategy, no curtailment occurs in this configuration, as the electricity supply is assumed to be fully controllable and unlimited. In this case, the TES and/or BESS are charged during the daytime and discharged during the following night, either through the PB or via direct feed-in to the grid from the battery. The cost of electricity from this fictional PV source is set to 20 \$/MWh_{el}, based on the cost of self-generated PV electricity provided by the plant operator and used as charging electricity price for the same plant in [32]. This approach eliminates the variability of the real solar resource, which is instead resolved in the Night-Real strategy, and enables direct comparison of the plant concepts under standardized charging and discharging conditions. It serves as a benchmark rather than as a business case.

Fig. 1 illustrates the approximate daily profiles corresponding to each operating strategy. It should be noted that the charge supplied varies from day to day, with significant seasonal variations, as well as changes in the number of nighttime hours.

2.2. Technical concepts

The five conversion concepts analyzed for the Angamos power plant are presented in detail below.

- **Hybrid CSP-PV plant with parabolic trough and thermal energy storage, coupled through an electric heater acting as a booster (called: Trough Hybrid)**

The first system (Fig. 2) analyzed in this study is a hybrid CSP-PV plant based on parabolic trough collectors coupled with a PV plant through an electric heater acting as a temperature booster. Hybrid power plants that combine photovoltaic and CSP technologies can achieve high flexibility and competitiveness by leveraging synergies between the two technologies. The PV field produces electricity at low cost during daytime, while the PT field provides thermal energy to a cost-effective molten salt TES. The stored thermal energy can be converted into electricity at night through the power block. This approach enhances the share of dispatchable renewable electricity, particularly during nighttime hours, which are critical for maintaining system adequacy in high-renewable grids.

Unlike conventional parabolic trough plants, which typically operate with synthetic oil as heat transfer fluid (HTF) and are limited to outlet temperatures of approximately 390 °C, the concept considered here integrates an electric heater capable of increasing the molten salt temperature up to 565 °C, matching the operating conditions of modern solar tower plants. This configuration allows the use of a mature and proven PT solar field technology while achieving higher storage and conversion efficiencies in the PB.

The electric heater introduces an additional degree of flexibility compared to a standard PT–PV hybrid plant. PV electricity during daytime can be directed to the EH, which increases the HTF temperature before entering the TES. This "booster" function increases the overall plant efficiency. Moreover, the EH provides a direct pathway for integrating surplus renewable electricity into the thermal storage, improving operational flexibility and grid support capability.

As described in the previous section, three operating strategies were defined for this configuration. It is necessary to establish the order of priority for the use of PV-generated electricity during daytime. This prioritization is not required for the third strategy (Night-Fict), since sufficient electricity is always assumed to be available to cover the auxiliary demand and to fully charge the thermal storage through the EH, without any direct PV feed-in to the grid.

- Baseload: During daytime, the PV electricity is used first to cover the plant's auxiliary power demand (e.g., pumping, tracking, control systems). Second, PV electricity is supplied to the EH in its booster function, increasing the molten salt temperature from the outlet of the oil–salt preheater, where heat from the parabolic trough field is transferred, up to 565 °C before entering the hot storage tank. Any remaining PV electricity is then exported to the grid. At night, the TES is discharged to generate electricity through the PB.
- Night-Real: In this strategy, PV electricity is not injected into the grid during daytime. Instead, it is first used to cover the auxiliary consumption of the plant and then directed to the EH in its booster function, heating the molten salts up to 565 °C to charge the TES. The stored energy is later converted into electricity in the PB during nighttime operation.
- Night-Fict: The PV electricity required to cover the auxiliary consumption of the plant and to supply the EH is assumed to be supplied by the hypothetical grid-connected PV source. The electric heater raises the molten salt temperature to 565 °C to fully charge the TES. The stored thermal energy is subsequently converted into electricity in the PB during nighttime operation.

- **Hybrid CSP-PV plant with solar tower and thermal energy storage, with an electric heater in parallel (called: Tower Hybrid)**

The hybrid PV–solar tower plant (Fig. 3) integrates a PV field with a central receiver tower system, an electric heater operating in parallel, and a molten salt TES. Tower technology inherently achieves higher operating temperatures (≈565 °C), which enhances the efficiency of the power block and reduces specific storage costs compared to parabolic trough systems without temperature boosting. The integration of the EH in parallel with the solar receiver enhances system flexibility, enabling continuous TES charging and stabilizing the receiver outlet temperature under fluctuating solar input. This hybrid configuration combines the high efficiency and storage performance of tower technology with the cost advantages and operational flexibility of photovoltaic generation.

As in the previous configuration, it is necessary to define the priority of PV electricity use during daytime for the Baseload and Night operational strategies.

- Baseload: During daytime, PV electricity is first used to cover the auxiliary demand of the plant (e.g., pumps, heliostat tracking, control systems). The remaining PV generation is then fed into the grid. Any surplus electricity beyond the grid export capacity is directed to the EH. In this configuration, the EH does not act as a booster (as in the parabolic trough case), but instead directly heats the molten salt from the cold tank temperature to the hot tank temperature, thus charging the TES. During nighttime, the TES is discharged, and the PB generates electricity from the stored thermal energy.
- Night-Real: In this strategy, PV electricity is not injected into the grid during daytime. It is first used to cover the auxiliary consumption of

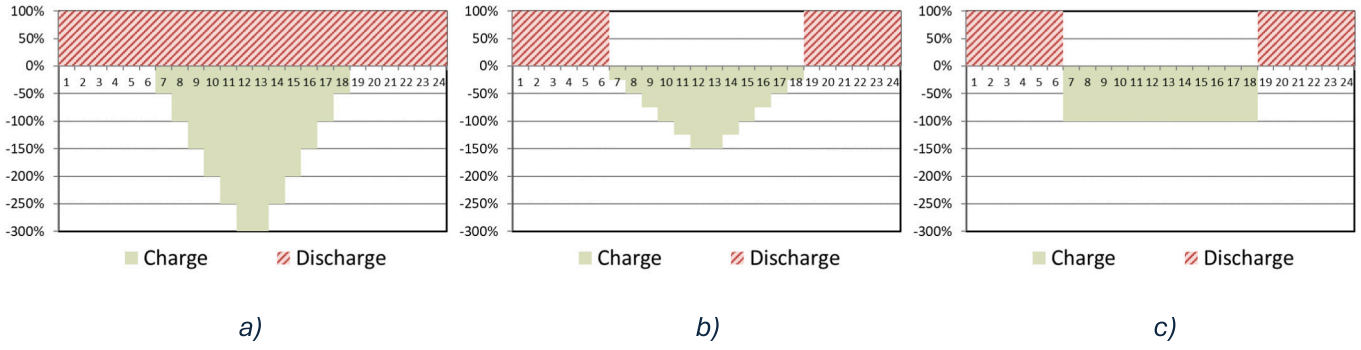


Fig. 1. Operating strategies: a) Baseload, b) Night-Real, c) Night-Fict.

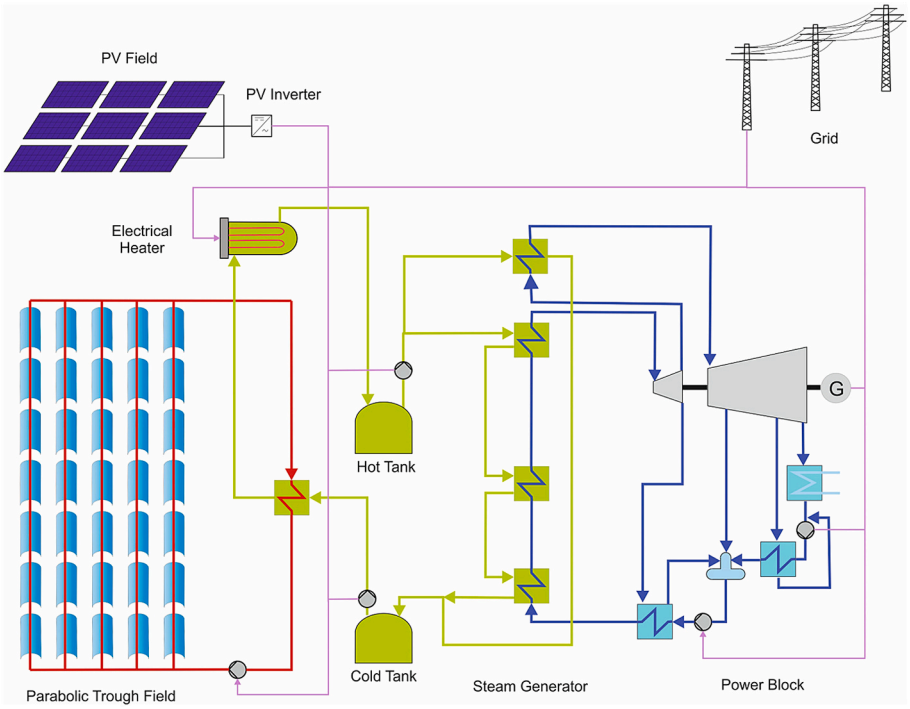


Fig. 2. Hybrid CSP-PV plant with parabolic trough and thermal energy storage, coupled through an electric heater acting as a booster (called: Trough Hybrid).

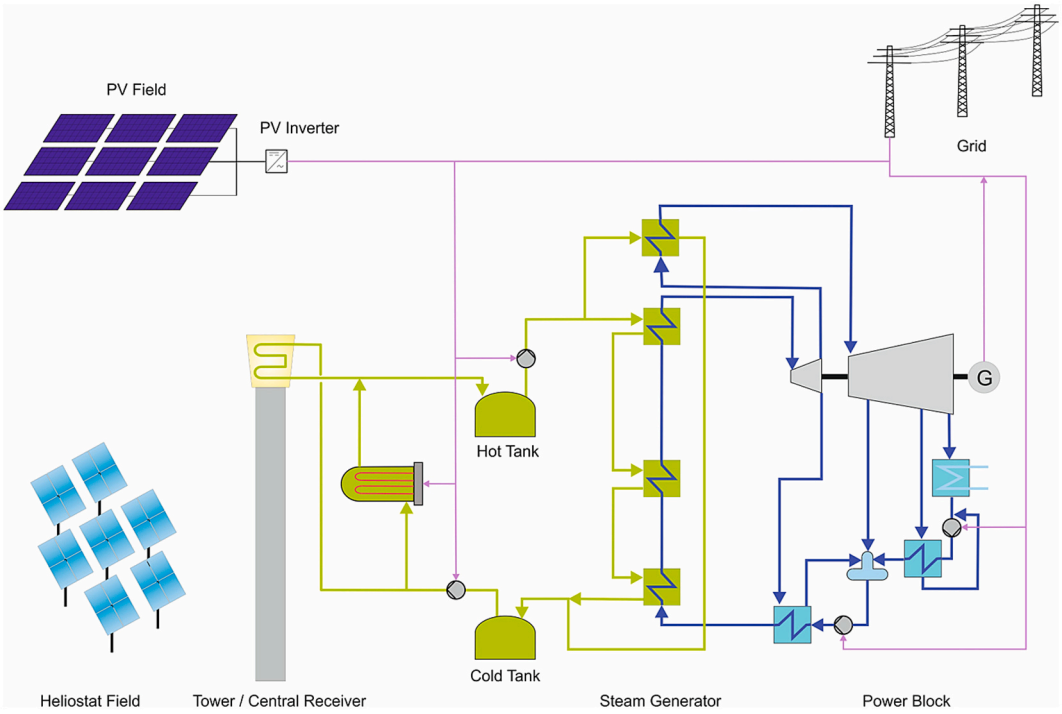


Fig. 3. Hybrid CSP-PV plant with solar tower and thermal energy storage, with an electric heater in parallel (called: Tower Hybrid).

the plant and then directed to the EH to charge the TES by heating the molten salts from the cold to the hot temperature. If the EH cannot absorb all available PV electricity, the excess is curtailed. At night, the TES is discharged, and the PB is operated to generate electricity from the stored heat.

- Night-Fict: The PV electricity required to cover the auxiliary consumption of the plant and to supply the EH is assumed to be supplied by the hypothetical grid-connected PV source. The EH directly heats the molten salt from the cold tank temperature to the hot tank temperature, fully charging the TES. The stored thermal energy is subsequently discharged during nighttime operation to generate electricity in the PB.

- **Standalone CSP solar tower plant (called: Tower)**

The standalone CSP tower configuration (Fig. 4) consists exclusively

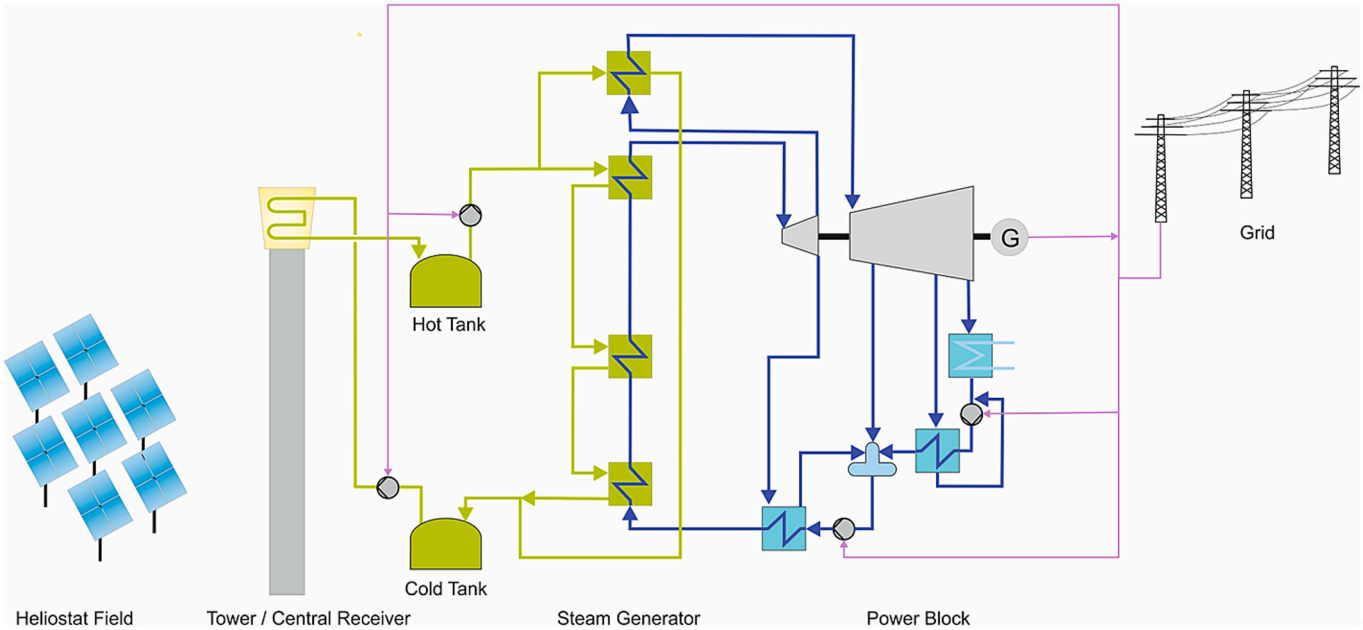


Fig. 4. Standalone CSP solar tower plant (called: Tower).

of a central receiver system, a molten salt TES, and a power block, without any coupling to a photovoltaic field. The tower receiver enables high operating temperatures of 565 °C, which allows for efficient power generation and cost-effective storage integration. This system represents a purely solar-thermal approach, relying entirely on direct normal irradiance (DNI) as the energy source.

The following individual assumptions apply to the operating strategy of the solar tower plant:

- Baseload: The PB is operated continuously during daytime whenever the CSP field can provide sufficient thermal power above the minimum load required for stable operation. The thermal energy collected by the receiver is prioritized for direct power generation in the PB. Any surplus thermal energy that cannot be immediately converted into electricity is stored in the TES, while during periods of insufficient DNI, the TES provides additional thermal input to stabilize PB operation. System optimization typically results in a CSP field large enough that the TES is mainly discharged at night. During nighttime hours, the stored energy in the TES is released to generate electricity through the PB.
- Night-Real: the PB is dispatched exclusively during nighttime hours, using the energy accumulated in the TES. During the day, the CSP field is fully dedicated to charging the thermal storage, with no electricity generation in the PB.
- Night-Fict: Not applicable, as no PV plant is included in this configuration.

- **PV plant with BESS (called: PV BESS)**

The PV BESS configuration (Fig. 5) consists of a PV plant coupled with a battery energy storage system, without any CSP integration. The BESS serves as an alternative storage technology, providing flexibility in electricity dispatch and enabling nighttime generation from stored PV energy.

For the PV BESS configuration, the following operating strategies are analyzed:

- Baseload: PV electricity is fed directly into the grid during daytime. Any surplus PV generation that cannot be immediately consumed is stored in the BESS. If the available storage capacity is fully utilized, the remaining surplus PV electricity is curtailed. During nighttime, the battery supplies electricity, allowing partial coverage of the continuous load curve. The integration of PV and BESS creates synergies by enabling flexible use of low-cost solar electricity while taking advantage of the high efficiency and fast response of modern battery systems.
- Night-Real: Electricity is dispatched exclusively at night using the BESS. During the day, the PV plant is fully dedicated to charging the battery. Surplus PV electricity is stored efficiently, and the battery ensures a stable nighttime supply.
- Night-Fict: The electricity required to charge the BESS is assumed to be supplied by the hypothetical grid-connected PV source, which provides constant and unlimited daytime generation. The battery is charged during the day and discharged at night to supply electricity to the grid.

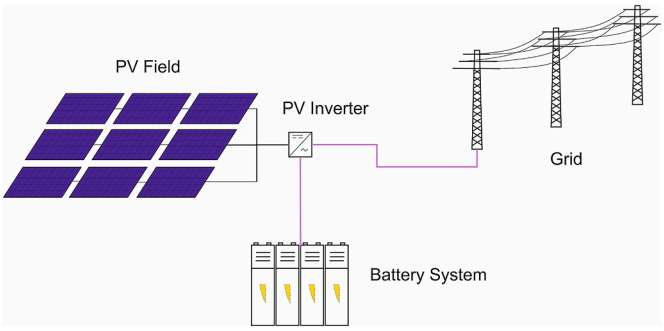


Fig. 5. PV plant with BESS (called: PV BESS).

- **Carnot battery plant (called: Carnot)**

The Carnot battery system (Fig. 6) consists of a PV plant coupled with a thermal energy storage system and an electric heater, without any CSP collectors. The EH converts electricity from the PV plant into thermal energy, which is stored in the TES and later reconverted into electricity through a power block during nighttime. This concept represents a

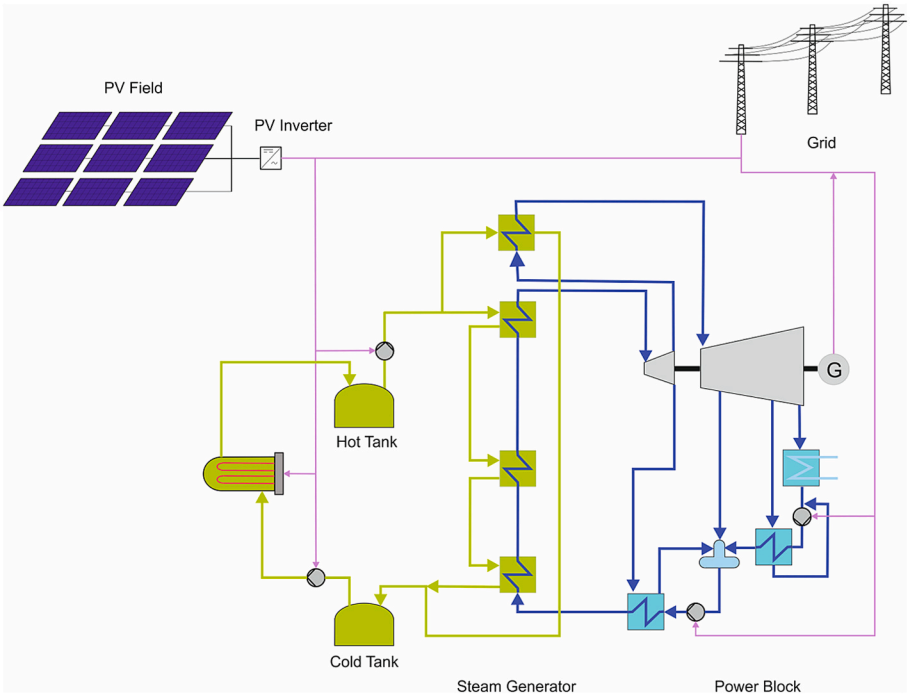


Fig. 6. Carnot battery plant (called: Carnot).

power-to-heat-to-power (P2H2P) system, providing a flexible and cost-effective means of dispatching renewable electricity.

For the Carnot battery configuration, the following operating strategies are considered:

- Baseload operation: PV electricity is fed directly into the grid during daytime. Surplus PV generation is redirected to the EH to charge the TES. This integration enables the system to make flexible use of inexpensive PV electricity while maintaining continuous operation and stabilizing the PB input conditions.
- Night-Real operation (with real PV): Electricity is produced exclusively at night using the PB, supplied by the thermal energy storage. During daytime, the PV plant charges the TES via the EH.
- Night-Fict: The electricity required to operate the EH and charge the TES is assumed to be supplied by the hypothetical grid-connected PV source, with constant daytime availability. The stored thermal energy is discharged during nighttime to generate electricity in the PB.

3. Materials and methods

3.1. Simulation tools used

The techno-economic analysis of energy systems requires the use of simulation tools. The software used in this study for simulating complete energy systems was greenius [39], developed by the DLR Institute of Solar Research, free of charge and user-friendly, capable of modeling various energy systems. The tool allows for techno-economic analysis by calculating the yield of a typical operational year, enabling the assessment of relevant economic parameters. All configurations simulated in this study, including all their components, are fully compatible with greenius.

The performance maps for simulating the power block in greenius were calculated using EBSILON® Professional [40], while the performance maps for the heliostat field and tower receiver were obtained using HFLCAL [41]. The HFLCAL optical model has been validated against ray-tracing calculations, with deviations in field efficiency of the order of 1% [41], and greenius has been validated against operational data from parabolic trough plants [39]. No coal-fired power plant has yet been retrofitted with a molten salt storage system, so a validation of the complete plant concept against operational data is not possible.

For all simulations, a typical meteorological year dataset from Angamos with a one-hour resolution was generated using Meteonorm [42] for the site coordinates. All components are evaluated at each time step as a function of the actual irradiance and ambient conditions. Monthly mean values of global horizontal irradiance are derived from ground station and satellite data, hourly series are generated from them by stochastic models, and the direct and diffuse components are separated using the Perez model, from which the direct normal irradiance is obtained [42].

In greenius, the power block is represented by a look-up table that returns the gross power output by interpolation over the thermal input and ambient conditions, so that part-load operation, start-up energy demand, and cool-down behavior are resolved. The solar fields are likewise modeled in greenius using the formulation appropriate to each technology, with the relevant loss mechanisms resolved at every time step. For the PV field these include the angle of incidence on the module plane, the module temperature and the inverter part-load efficiency; for the parabolic trough field, longitudinal and transversal incidence angle modifiers, cleanliness and availability, and the thermal losses of the absorber and the piping; and for the heliostat field, the solar-position-dependent optical efficiency and the receiver losses. Dumping is accounted for when the available heat exceeds the capacity of the storage or the power block.

3.2. Conversion of the Angamos coal-fired power plant

This study focused on the techno-economic analysis of converting the Angamos coal-fired power plant in Chile into various renewable concepts utilizing solar generation and energy storage. The existing power block of each unit at Angamos is reusable and serves as a reference for simulation and techno-economic analysis.

The Angamos coal-fired plant is located in Mejillones, in the Antofagasta region of northern Chile. Commissioned in 2011, the plant still has a significant remaining operational life and is operated by AES

Andes S.A. It consists of two power units, which operate on coal. In the original coal-fired design, the plant operates with live steam conditions of 565 °C and 160 bar, a gross efficiency of 44.2%, and a gross power output of 277 MW_{el}. The boiler efficiency is 87.5%, and the cooling water temperature is 28 °C.

For simulating this power block in the proposed renewable concepts, it was modeled in EBSILON® Professional (Fig. 7). The model was built from the detailed heat balance diagrams provided by the plant operator and validated against them. The same power block has been modeled with the same tool in previous work [31]. Performance maps were generated for operation under various conditions and subsequently integrated into greenius for the simulation of the complete renewable plants. In the simulation, the coal-fired plant produced a net output of 250.9 MW_{el}, which was adopted as the net power for the power block in the new renewable concepts, corresponding to a gross efficiency of 43.5%. In the renewable configurations the power block is operated with live steam at 560 °C, specified by the plant operator for the retrofit; the performance maps used in greenius were generated for these conditions. The molten salt temperature range of 565 °C to 300 °C was verified to maintain a minimum temperature difference of 5 K across the salt steam generator under nominal design conditions. Fig. 7 shows the EBSILON® Professional model of the Angamos coal-fired plant.

For the techno-economic analysis of the energy systems, two approaches were considered. The first, a "brownfield" approach, involves using the existing Angamos power block in the new plants. The second, a "greenfield" approach, entails installing a completely new power block. In both cases, the same performance maps calculated in EBSILON® Professional were used for the simulation in greenius.

When converting the coal plant into a solar-based plant, the meteorological and geographical data of the site become important, as summarized in Table 1. Solar radiation is lower than expected for this latitude due to the plant's proximity to the sea.

Table 1
Main meteorological and geographical parameters of Angamos site.

Parameter	Value
Annual DNI (TMY) [kWh/m^2]	2359
Annual GHI (TMY) [kWh/m^2]	2179
Average Temperature [°C]	16.6
Latitude [°S]	23.07
Longitude [°W]	70.37
Altitude [m]	49

3.3. Evaluation criteria

A techno-economic analysis requires well-defined evaluation criteria to enable a meaningful comparison of different technologies. As the main economic criterion, the Levelized Cost of Electricity (LCOE) was employed, as it is a straightforward and widely used metric in comparative energy technology studies. It represents the average cost per unit of electricity generated over the system's lifetime, allowing the assessment of different plant concepts under uniform economic conditions. Eq. (1) shows the formula used in this study for its calculation:

$$\mathrm{LCOE} = \frac{\text{Total Investment Costs} + \sum_{t=1}^{t_{ges}} \frac{\text{Annual Running Costs}_t}{(1+r)^t}}{\sum_{t=1}^{t_{ges}} \frac{\text{Annual Electricity Solar}_t \times (1-d)^{t-1}}{(1+r)^t}}, \quad (1)$$

where r is the interest rate, t is the year within the period of use (1, 2, … t_{ges}), t_{ges} is the system lifetime in years, and d is the annual degradation rate, applied to the electricity generated from the solar resource, for which the same value is assumed for PV and CSP (Table 2). The degradation of the BESS is treated separately and compensated through the operating costs, as described in Section 3.5.

However, the LCOE alone is not sufficient to evaluate the performance of energy systems. A second indicator is necessary to quantify the amount of electricity generated during nighttime hours. The goal of this study is not only to minimize costs but also to maximize dispatchable nighttime generation. Without this additional metric, a PV-only system without storage would appear economically optimal but would not provide any nighttime electricity supply. To capture this complementary aspect, three additional indicators were used in the analysis. Each of them provides relevant information, and none is entirely free of limitations:

- Capacity factor: Shows how much electricity is produced in a year relative to the theoretical maximum if the plant is operated at full capacity continuously. However, it does not indicate when the generation occurs. A high capacity factor could correspond entirely to daytime production. It is calculated according to Eq. (2):

$$\text{Capacity factor} = \frac{\text{annual gross electricity production}}{\text{nominal power} \times 8760} \quad (2)$$

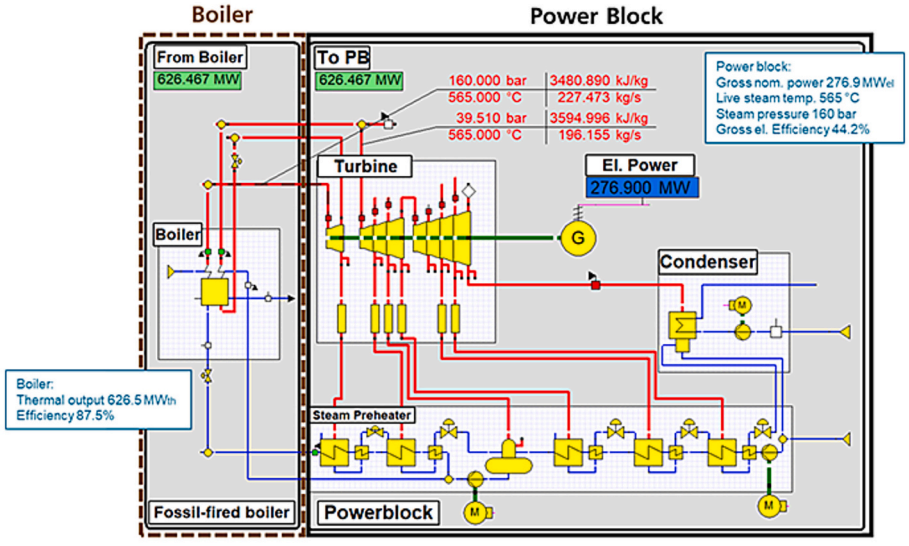


Fig. 7. Detailed system process model for the Angamos coal-fired power plant.

Table 2
Technical assumptions.

Technology	Technical assumptions
Parabolic trough (PT)	Collector type: Ultimate Trough (Aperture width: 7.51 m, collector length: 246.7 m, effective mirror area: 1716 m^2, heat collection element diameter: 8.9 cm, Nominal optical efficiency: 82.7%). Distance between rows: 22.5 m; Distance between collectors: 0.5 m HTF: Therminol VP-1 Nominal field outlet temperature: 393 °C Nominal field inlet temperature: 300 °C Degradation: 0.4% per year
Solar tower (ST)	HTF: Solar Salt (60% $NaNO_3$, 40% KNO_3) Nominal tower outlet temperature: 565 °C Nominal tower inlet temperature: 300 °C Degradation: 0.4% per year
PV	Bifacial-monocrystalline PV modules Single-Axis Tracking Systems DC/AC ratio: 1.3 PV panels nominal efficiency: 19% PV inverter nominal efficiency: 98.6% Degradation: 0.4% per year Assumption: Optimized standalone PV configuration will also lead to the highest benefits in integrated hybrid plants. A representative single inverter system was designed and in the hybrid plants many of these systems were used to achieve the required nominal power.
Power2Heat technology: electric heater (EH)	HTF: Solar Salt (60% $NaNO_3$, 40% KNO_3) Technology: electric resistance heater Conversion efficiency: 99%
Thermal energy storage (TES)	Storage Medium: Solar Salt (60% $NaNO_3$, 40% KNO_3) Nominal hot temperature: 565 °C Nominal cold temperature: 300 °C Thermal energy losses: 1% per day [43]
Power block (PB)	Gross capacity: 268 MW_{el} Net capacity: 250.9 MW_{el} Gross efficiency at 100% load: 43.5% Gross efficiency at 50% load: 38.2% Live steam temperature: 560 °C Live steam pressure: 160 bar Hot reheated steam temperature: 560 °C Hot reheated steam pressure: 40 bar Exhaust steam temperature: 41 °C Exhaust steam pressure: 78 mbar Feedwater temperature: 261 °C Cooling water temperature: 28 °C
Battery energy storage system (BESS)	Technology: Lithium-Ion Nickel Manganese Cobalt Round-trip efficiency: 85% related to heating, ventilation and air conditioning, self-discharge, battery management system, power conversion system efficiency, etc. Lifetime (warranty period): 15 years (BESS has to be completely replaced after 15 years, Operations and Maintenance (O&M) cost assumption includes a share to build up an O&M budget for the replacement) Degradation: ≈2% of nominal capacity per year (lost BESS capacity must be restored by adding additional batteries on a regular basis to maintain BESS functionality, O&M cost includes a share to compensate degradation) [13]

- Night Capacity Factor: Measures the amount of electricity produced during nighttime hours (see Fig. 8) relative to the maximum possible generation during those hours. It directly indicates how effectively the system delivers dispatchable energy at night, but it does not account for the plant's total energy production over the full day. Its value is obtained from the ratio defined in Eq. (3):

$$\text{Night capacity factor} = \frac{\text{annual nighttime electricity production}}{\text{nominal power} \times \text{nighttime hours per year}} \quad (3)$$

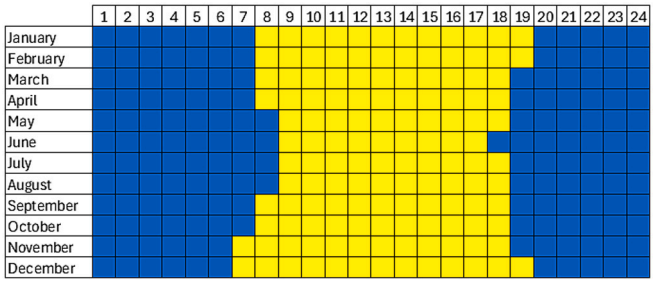


Fig. 8. Daytime (yellow) and nighttime (blue) hours for each month of the year. (For interpretation of the references to colour in this figure legend, the reader is referred to the web version of this article.)

- Nighttime Electricity Fraction: Describes the proportion of total annual electricity generation that occurs during nighttime. However, it provides no information about the absolute generation volume or plant utilization. Its calculation is shown in Eq. (4):

$$\text{Nighttime electricity fraction} = \frac{\text{annual nighttime electricity production}}{\text{total annual electricity production}} \quad (4)$$

To calculate these indicators, it was necessary to define which hours of each day are considered nighttime. This was determined for the Angamos site on a monthly basis. An hour was defined as nighttime if, on a clear-sky day in the middle of the month, the PV output did not reach 25% of its nominal value for that hour. This definition was then applied to all days of the corresponding month. The meteorological datasets were evaluated with a time resolution of one hour. Fig. 8 illustrates the daytime (yellow) and nighttime (blue) hours defined for each month of the year. As the criterion is evaluated on a monthly basis, the number of nighttime hours per day varies over the year, from 11 h in December to 14 h in June, so that the nighttime hours per year in Eq. (3) reflect this seasonal variation.

3.4. Technical assumptions

The technical assumptions for each component of the different power plant concepts are summarized in Table 2 and were defined based on [13,14], with the exception of the power block, which was derived from Angamos power plant [32], ensuring that methodology and comparability remain consistent with previous publications. The size of the components is modified in the parameter variation (see Section 3.6) in order to identify the configurations that best meet the evaluation criteria.

The limit of electrical feed-in to the grid was set at 250.9 MW_{el} for all systems, including both the power block and the net battery output, corresponding to the nominal net capacity of the Angamos power plant. This approach also simplified the design of the photovoltaic plant and allowed for consistent comparison between all concepts. The gross power of the power block was defined to ensure coverage of all auxiliary demands under all operating conditions and to achieve the net output of 250.9 MW_e. The load curve was assumed to remain constant at 250.9 MW_{el} either throughout the day (baseload operation) or during nighttime hours only (storage-based operations). Auxiliary demands were defined as either temperature-dependent or fixed, depending on the component. Connections to the grid, substations, and transmission lines were not included in the project scope. This approach enabled a direct comparison of all plant concepts independently of location, without considering site-specific electrical connections.

3.5. Cost assumptions

The cost assumptions applied to the various system components are

shown in Table 3. These values were derived from [13,14]. Although the data correspond to 2021, they provide a consistent and referable basis that allows for a consolidated methodology in the techno-economic comparison of technologies. Moreover, the limited deployment of CSP plants in recent years has introduced additional uncertainty when assuming costs. Therefore, the results should be interpreted primarily in relative terms, emphasizing the differences between system concepts rather than absolute investment figures. Engineering, procurement, and construction (EPC) surcharges were linked to capital expenditure (CAPEX) and estimated using different values for each subsystem, reflecting the differing levels of technological maturity.

Costs related to permitting, land use, and site-specific civil works were not included, as their contribution was considered minor relative to the main plant investment costs: the plant is located in a sparsely populated desert area on an existing industrial site, where land is available and already designated for power generation. An interest rate of 5% and an operational lifetime of 25 years were assumed jointly with Dornier Suntrace within the framework of [13], based on practical experience in several renewable energy projects, including CSP. The 5% real discount rate is a common reference value in comparative techno-economic studies [13,14]. The lifetime of 25 years corresponds to the design lifetime typically applied to CSP plants. In the brownfield cases, the Angamos power block was commissioned in 2011, so that a further 25 years of operation would imply a total service life of approximately 40 years, which is within the range routinely achieved by steam turbine-generator sets subject to normal overhaul.

The treatment of BESS degradation given in Table 2 follows the approach adopted in [2], where the fixed O&M is assumed to counteract degradation such that the system performs at rated capacity throughout its lifetime; the assumed O&M share, lifetime and round-trip efficiency are consistent with that reference. The degradation rate therefore affects the cost side of the LCOE rather than the electricity yield, and is not applied to BESS electricity in Eq. (1).

Two approaches were followed for calculating power block costs. In the brownfield case, no new power block investment is considered; however, costs related to the integration of the existing Angamos power block with the new plant components, as well as the installation of a new molten salt steam generator (SG) including its reheat section, are included. The integration cost was estimated at 10 $/kW$_{th}$ for the Angamos site within the prefeasibility assessment carried out in [32]. In the greenfield case, the full cost of a newly built power block is accounted for. This comparison enables a direct assessment of the impact of power block reuse on the overall economics. The operating costs of the power block account for the daily start-up required in the storage-based configurations, based on a conservative estimate made together with the plant operator in [32].

Table 3
Cost assumptions.

Technology	Component	Value 2021	Unit
PT	Solar field	202	$/m^2
	EPC	0.2	of CAPEX
	O&M	0.015	of CAPEX
ST	Heliostat field	127	$/m^2
	Tower	88,000	$/m
	Receiver	122	$/kW$_{th}$
	EPC	0.2	of CAPEX
	O&M	0.015	of CAPEX
PV system	Inverter	53	$/kW$_{ac}$
	PV field	454	$/kW$_{dc}$
	EPC	0.1	of CAPEX
	O&M	0.005	of CAPEX
EH	EH	100	$/kW$_{el}$
	EPC	0.2	of CAPEX
	O&M	0.01	of CAPEX
TES	Thermal storage	26	$/kWh$_{th}$
	EPC	0.2	of CAPEX
	O&M	0.015	of CAPEX
PB	Greenfield (incl. SG + integration)	966	$/kW$_{el}$
	Brownfield (only SG + integration)	210	$/kW$_{el}$
	EPC	0.2	of CAPEX
	O&M	0.015	of CAPEX
BESS	Cost per power	245	$/kW$_{el}$
	Cost per energy capacity	246	$/kWh$_{el}$
	EPC	0.235	of CAPEX
	O&M	0.045 (see Table 2)	of CAPEX

3.6. Parameter variation

A parameter variation was conducted for each energy system to identify specific configurations that yielded the lowest LCOE for each of the simulated storage capacities. These storage capacities were 3 h, 6 h, 9 h, 12 h, and 15 h. With storage capacities of up to 15 h, the aim was to analyze, for each technology, storage sizes that could cover the entire nighttime demand.

The varied parameters included the PV field size, the CSP field size, and the electric heater nominal power for each storage capacity. The steps and limits applied in the parametric variation are summarized in Table 4; they were selected as a compromise between resolution and computational effort, as finer increments were verified not to change the results significantly. Within the ranges investigated, the resulting LCOE variations are below 0.001 $/kWh. Parametric variation produces a very large number of results. Configurations with the lowest LCOE for each storage capacity were selected for visual representation of the results. The parabolic trough field is varied in steps of one collector loop, which corresponds to 27.7 MW$_{th}$; thermal power is reported here for comparability with the other configurations.

4. Results and discussion

The parametric variation resulted in a large number of simulation outputs, which required a selection process to ensure clear and comprehensible visual representation. The simulations covered five different energy system configurations, three operational strategies, and two scenarios regarding the reuse of the existing power block (brownfield, greenfield). Each of these scenarios was analyzed for five different storage capacities. For clarity, only those parametric configurations yielding the lowest LCOE for each storage capacity were selected for graphical representation. These representative cases provide an optimized comparison among technologies. In this study, the selected scenarios are presented in grouped diagrams, where the different technologies are compared according to the defined evaluation criteria.

Table 4
Steps and limits of the parameter variation.

Technology	PV field size [MW$_p$]	Storage net capacity [h]	CSP field nominal power [MW$_{th}$]	EH nominal power [MW$_{el}$]
Trough Hybrid	150–750 (25 MW step)	3–15 (3 h step)	28–554 (28 MW step)	10–1000 (variable step)
Tower Hybrid	250–1000 (25 MW step)	3–15 (3 h step)	200–400 (50 MW step)	10–1000 (variable step)
Tower	–	3–15 (3 h step)	200–2800 (50 MW step)	–
PV BESS	250–750 (25 MW step)	3–15 (3 h step)	–	–
Carnot	250–1750 (25 MW step)	3–15 (3 h step)	–	10–1000 (variable step)

4.1. Brownfield scenario

Fig. 9 presents the LCOE of all analyzed technologies and operating strategies as a function of the capacity factor for the Brownfield scenario, in which the existing power block of the Angamos plant is reused. This assumption leads to lower total investment costs for all systems that include this component. As the primary objective of this study is the analysis of the Angamos power plant conversion, the brownfield scenario is taken as the baseline case.

The analysis of Fig. 9 shows that the Carnot battery and the hybrid CSP-PV systems (i.e. Trough Hybrid, Tower Hybrid) achieve very similar LCOE values across all operational strategies, particularly for the Carnot battery and the Tower Hybrid configuration. The Trough Hybrid system exhibits slightly higher values under the storage-based operating modes (Night-Real and Night-Fict). The standalone Tower plant displays comparatively higher costs, especially in baseload operation, while the difference becomes less pronounced under the Night-Real strategy, where the LCOE is only slightly higher.

A direct comparison between the Carnot battery and the standalone Tower under the Night-Real strategy isolates the cost of heat generation from PV + EH versus that of the solar tower. This is possible because both configurations are assumed to share equivalent TES and PB CAPEX and O&M and deliver electricity to the grid exclusively through the PB during nighttime operation. The higher LCOE of the standalone Tower indicates that the cost of thermal energy generation is slightly lower in the PV + EH configuration. This explains why the Carnot battery achieves the lowest costs among the storage-based systems, benefiting from cheaper heat production. The Tower Hybrid system reaches very similar costs. This occurs because the parametric variation yields configurations with the lowest LCOE for each storage capacity at or near the minimum tower nominal power of 200 MW_{th} investigated (Table 4). Consequently, the Tower Hybrid data points in storage-based operation (Night-Real and Night-Fict) correspond to designs that are effectively similar to the Carnot battery. Since a small tower size and only slightly higher heat-generation costs have limited influence on total plant costs, the resulting LCOE remains close. In baseload operation, larger towers of around 300 MW_{th} are obtained for storage capacities of 12–15 h. This results from the fact that PV electricity is fed into the grid during the day, while additional electricity is required to operate the electric heaters that charge the TES. To maintain high utilization of these heaters and avoid an increase in heat-generation costs, the tower provides complementary thermal input, which reduces overall costs once the plant reaches a certain scale compared with the PV + EH combination. In any case, the costs of both systems remain comparable, and the PV field in the hybrid-tower system is large. It should also be noted that the resolution of the parametric variation influences which configurations are selected as optimal; a finer resolution might shift the selected designs slightly without a relevant effect on the LCOE (see Section 3.6).

The standalone Tower plant in the baseload strategy shows distinctly higher LCOE than the Trough Hybrid, Tower Hybrid and Carnot systems because it cannot benefit from the low-cost PV electricity generated during daytime. In the Night-Real strategy, this advantage disappears, so the Tower's LCOE becomes only slightly higher, consistent with the similar heat-generation costs.

The costs of the Trough Hybrid system are slightly higher than those of the Carnot battery and Tower Hybrid systems. Its capacity factor is also somewhat lower due to the coupling between the CSP and PV fields, which makes the storage charging more dependent on the DNI and slightly reduces the operating hours of the electric heater.

In contrast, the PV BESS configuration shows higher LCOE but also the highest capacity factors across all operational strategies, particularly under baseload and Night-Real operation. The elevated costs are primarily due to the higher cost of battery storage compared with thermal storage, which is also reflected in the upward slope of the LCOE curve with increasing storage capacity in baseload operation, a trend not observed for the other systems. This difference in behavior follows from the magnitude of the cost difference: the marginal cost of storage capacity is 26 $/kWh$_{th}$ for the TES-based concepts against 246 $/kWh$_{el}$ for the BESS, almost an order of magnitude higher, so that beyond a certain capacity the additional investment outweighs the additional yield. Moreover, PV BESS is the only configuration that does not benefit from the Brownfield scenario, since the existing power block cannot be reused. The high capacity factors arise from the relatively low cost of PV generation, which economically justifies oversizing the PV field to

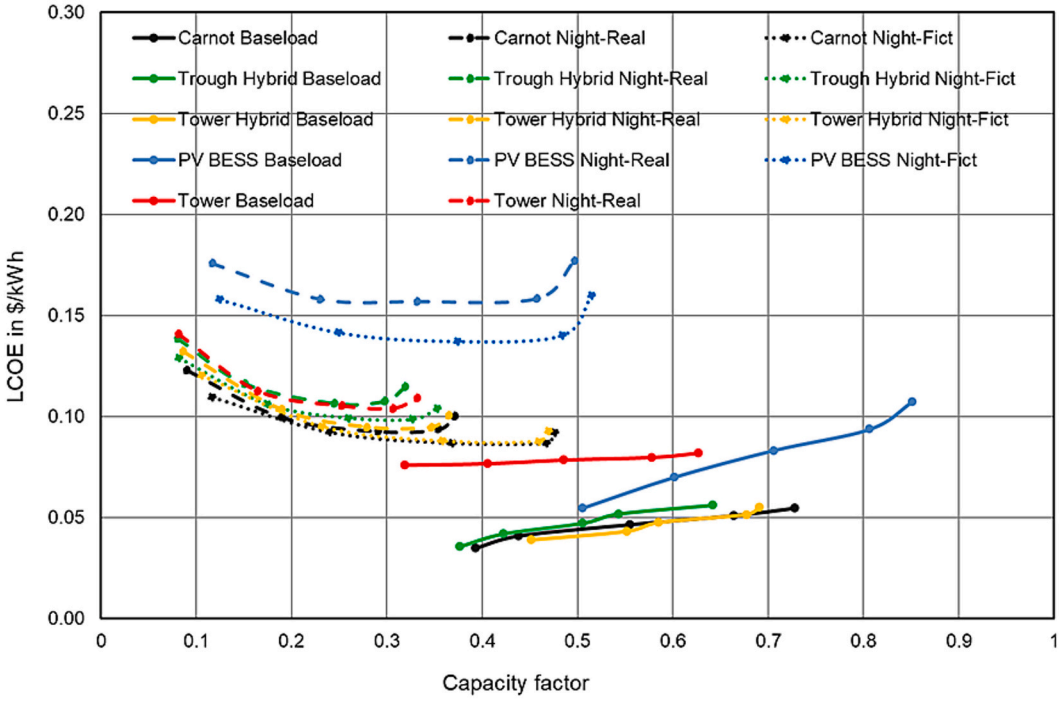


Fig. 9. LCOE versus capacity factor for different technologies and operating strategies (Brownfield scenario).

improve battery utilization.

Overall, the results confirm a strong dependence on the underlying cost assumptions. The differences in heat generation costs between the Tower Hybrid and the Carnot (i.e., PV + EH systems) are relatively small, such that minor variations in the assumed costs could affect the optimal design choices. Similarly, the ranking of parabolic-trough technology is also sensitive to cost assumptions. These observations highlight the importance of further exploring how changes in component costs influence system performance, which is addressed in the sensitivity analysis.

When comparing baseload and Night-Real operation, the Night-Real operation results in higher LCOE because electricity can be produced for the grid only during nighttime hours, reducing overall utilization. In addition, low-cost PV electricity cannot be exported to the grid during daytime. Since PV generation during the day is inexpensive, systems in Night-Real operation no longer benefit from it. The optimal design of the PV field is also more difficult due to dumping effects when the storage becomes full. The LCOE gap between the hybrid systems and the standalone tower decreases under Night-Real operation, as the tower's heat-generation costs are similar in both strategies and it cannot benefit from PV-based daytime production in baseload. However, the relative LCOE difference with PV BESS increases further in Night-Real operation because of the much higher cost of battery storage compared with thermal storage. Capacity factors decrease for all systems, as electricity is produced only during approximately half of the annual hours, limiting the maximum achievable values. Therefore, the representation of additional indicators, such as the night capacity factor and nighttime electricity fraction, is necessary to allow a more balanced comparison between strategies.

Finally, introducing a fictional PV plant in the Night-Fict strategy, which provides an unlimited and constant daytime electricity supply at a fixed cost of 20 $/MWh$_{el}$, results in a significant reduction of LCOE, particularly for PV BESS systems. In this case, each component draws only the electricity required for its operation, enabling smaller and less expensive system sizing (e.g., reduced electric heater capacity) and eliminating dependence on variable solar irradiance. This is equivalent to allowing a smaller PV field without reducing total production, thereby lowering overall costs and eliminating curtailment effects. The PV BESS system benefits the most from this strategy, as its generation relies directly on the PV field. In addition, the constant electricity supply improves the utilization of the electric heater, lowering its cost per unit of energy produced annually.

Fig. 10 replaces the total capacity factor on the horizontal axis with the night capacity factor, offering further insights into the results. The night capacity factor is higher for the storage-based strategies (Night-Real and Night-Fict) than for the baseload case, since the optimal designs in these modes aim for maximum utilization during the limited nighttime hours to reduce generation costs. In baseload mode, daytime generation is cheaper. Therefore, increasing plant size to achieve a higher nighttime factor is not always economically justified, as it can raise component costs without sufficient gain in electricity production.

Systems with PV-based generation show higher night capacity factors than those with a stronger CSP component, particularly in the PV BESS configuration, which reaches the highest nighttime values for both Night-Real and Night-Fict operating strategies. This is a consequence of the high battery storage cost, which drives optimization towards maximum utilization and larger PV fields to reduce the nighttime generation cost.

For systems using thermal storage, night capacity factors with Night-Real strategy reach 65–75%, depending on the PV contribution, with higher values for configurations that can better exploit low-cost PV electricity. The Night-Fict strategy leads to a clear increase in night capacity factors, especially for the Carnot battery and Tower Hybrid systems. In the PV BESS system, the improvement is smaller, as storage is already used near its limit, with only marginal additional charging possible in the early and late daylight hours. The Carnot battery and Tower Hybrid, however, benefit substantially, since the constant electricity supply allows higher utilization of the TES without increasing total plant CAPEX. With this strategy, the constant PV production enables a reduction in electric-heater size for the same annual generation, thus further reducing investment costs. The Trough Hybrid system shows a less pronounced increase in night capacity factor because its PV electricity demand remains linked to the CSP field in the booster configuration and, therefore, to solar radiation. As a result, larger system

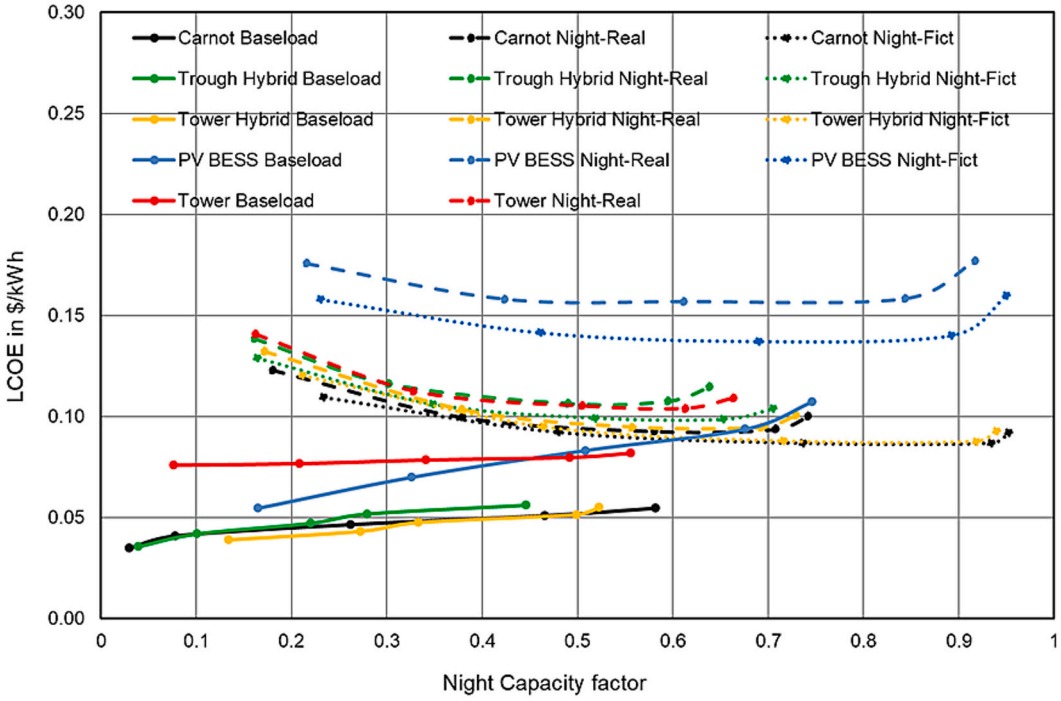


Fig. 10. LCOE versus night capacity factor for different technologies and operating strategies (Brownfield scenario).

sizes lead to stronger dumping effects once storage is full, limiting optimization potential. For comparison, the fixed cost of purchased PV electricity in the Night-Fict strategy is 20 $/MWh$_{el}$, while the real PV-only system (without storage) at Angamos would have a LCOE of 21.1 $/MWh$_{el}$. The difference between these two cases lies in the availability profile rather than in the price level: in the real PV-only system, output depends directly on solar irradiance, which prevents the same degree of optimization and cost reduction enabled by a constant electricity supply.

It should be noted that a lower night capacity factor in some systems does not imply technical infeasibility of reaching higher nighttime utilization, but rather that the optimal parametric design minimizes costs for a given storage capacity rather than maximizing nighttime output. Extending the result curves towards higher night capacity factors would be possible by increasing component sizes, but this would also raise the LCOE. Such a representation was not pursued in this study.

Fig. 11 uses the nighttime electricity fraction as the evaluation parameter, providing another perspective on system behavior. The PV BESS configuration exhibits a high nighttime electricity fraction because the combination of high storage cost and low PV generation cost drives strong battery utilization and, consequently, a high overall capacity factor with a substantial nighttime share. The higher nighttime fraction of the standalone Tower relative to hybrid systems (Trough Hybrid, Tower Hybrid) and Carnot is only apparent, since its total capacity factor is lower while the absolute nighttime production remains similar. The absence of a PV field producing inexpensive daytime electricity prevents the optimization from oversizing the generating field, thus reducing total capacity factor and nighttime electricity fraction.

4.2. Greenfield scenario

The Brownfield scenario, which assumes the reuse of the existing Angamos power block, was compared with a Greenfield scenario at the same site, in which a new power block is constructed. Fig. 12 presents the results of all energy systems and operating strategies as a function of the capacity factor, while Fig. 13 shows the corresponding results with respect to the night capacity factor.

The immediate effect of the Greenfield scenario is a general increase in the LCOE for all systems except the PV BESS, since it is the only configuration that does not include a power block. Consequently, the cost difference between PV BESS and the other systems decreases, and for a storage capacity of 3 h, PV BESS becomes the least-cost alternative for all operating strategies. In the greenfield scenario, the LCOE curves of the PV BESS and the hybrid and Carnot systems intersect at around 4–5 h of storage, a crossover that does not occur in the brownfield scenario.

In the storage-based strategies (Night-Real and Night-Fict), a pronounced increase in LCOE is observed for systems with power blocks when the storage capacity is limited to 3 h. In these cases, the fixed investment cost of the power block is distributed over a relatively small annual electricity production, since there is no daytime operation. As a result, the effective utilization of the power block is low, leading to higher specific generation costs.

Retrofitting existing infrastructure in a brownfield configuration significantly reduces the overall capital cost, making systems that include a power block, such as hybrid CSP-PV or Carnot battery concepts, more economically competitive. In contrast, under the greenfield scenario, total investment costs increase substantially, resulting in similar competitiveness to PV BESS systems. Moreover, the competitiveness of CSP technologies is strongly dependent on the available DNI. The Angamos site, located near the coast, is affected by the marine atmospheric layer, which suppresses direct irradiation relative to inland locations of the Atacama Desert. With a DNI of 2359 kWh/m^2/y and a DNI/GHI ratio of 1.08, the site receives about 32% less direct irradiation than an inland location in the Atacama Desert such as Diego de Almagro (3477 kWh/m^2/y, DNI/GHI ratio of 1.42) [42]. The site remains suitable for CSP deployment, and its DNI is comparable to or higher than that of established CSP locations in Spain and Morocco, but it does not offer the resource advantage of inland Atacama sites. This is inherent to the brownfield approach adopted here, since Chilean coal-fired power plants are located on the coast for cooling water supply and coal import logistics. As a consequence, the site conditions are comparatively more favorable for PV than for CSP, which is relevant for the comparison of concepts presented in this study.

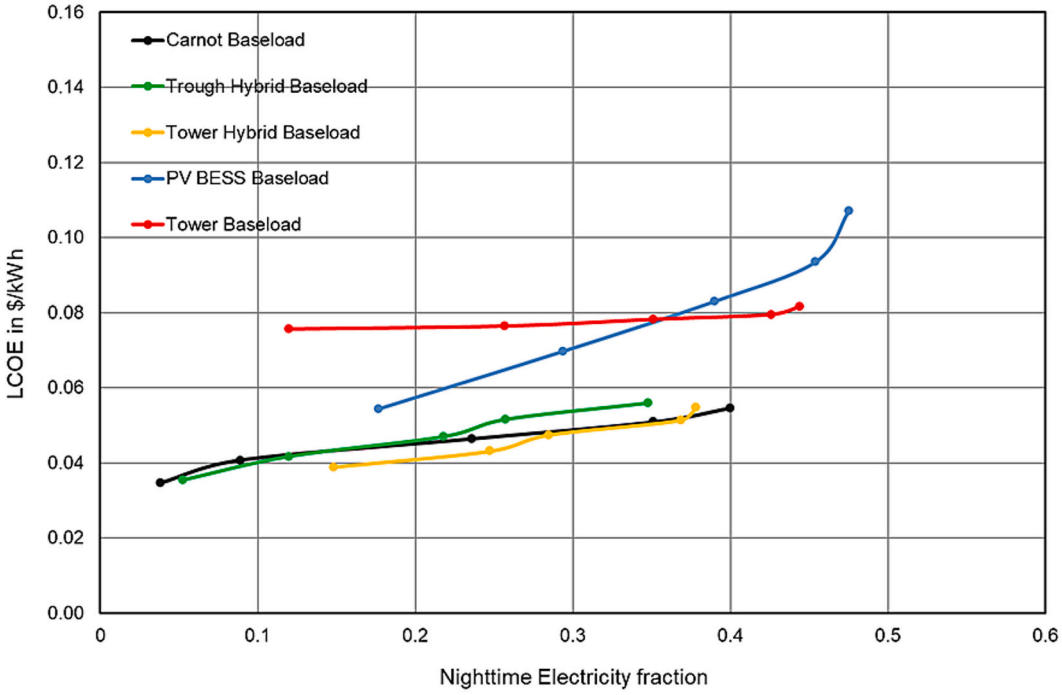


Fig. 11. LCOE versus nighttime electricity fraction for different technologies and operating strategies (Brownfield scenario).

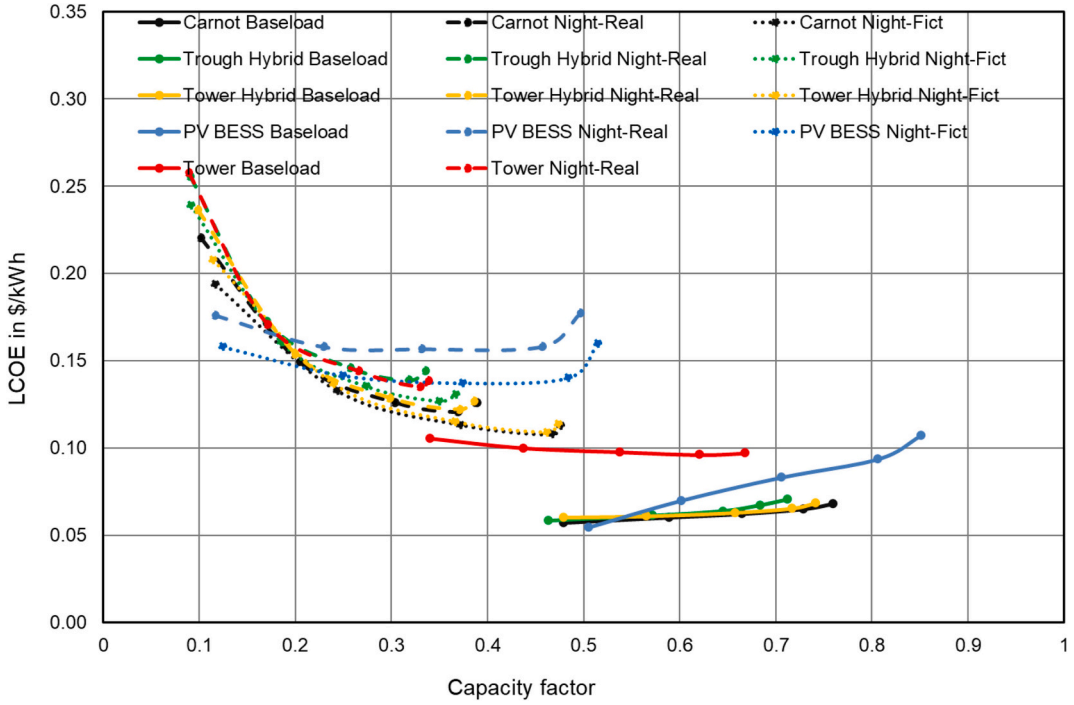


Fig. 12. LCOE versus capacity factor for different technologies and operating strategies (Greenfield scenario).

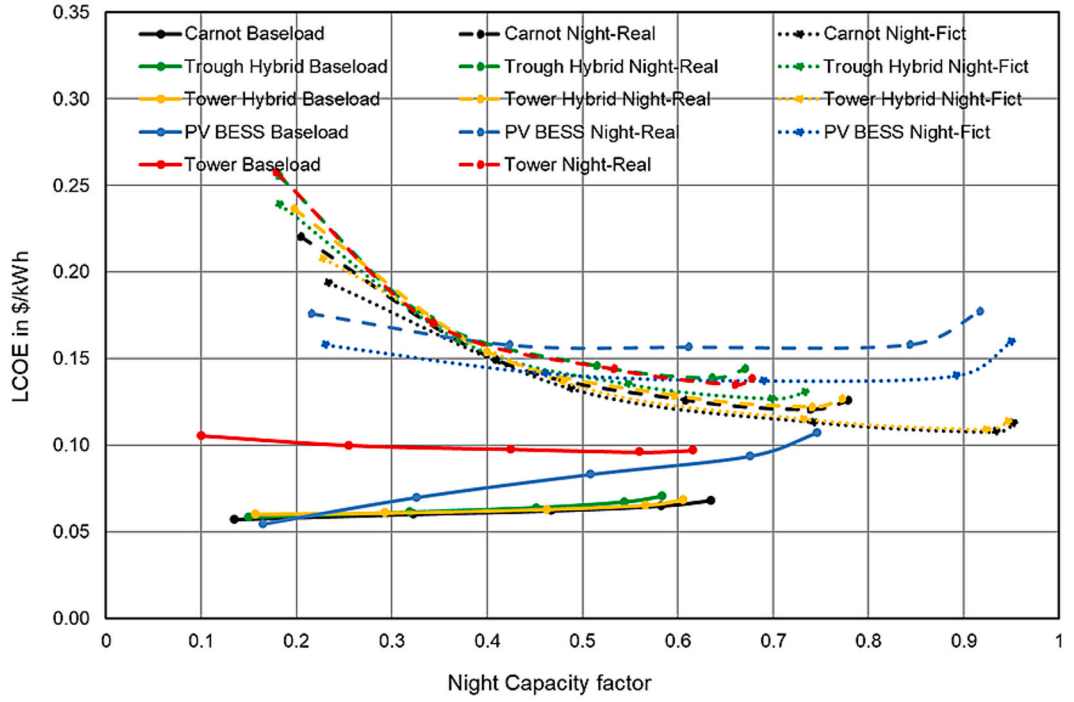


Fig. 13. LCOE versus night capacity factor for different technologies and operating strategies (Greenfield scenario).

4.3. Analysis of optimized plant designs

The comparison between the optimized parametric configurations of the different energy systems for specific storage capacities and operating strategies provides additional insight into their design characteristics and cost structures. Table 5 summarizes, as an example, the key parameters of the lowest-LCOE configurations with 6 h of storage, Night-Real operation, and the Brownfield scenario. Table 6 presents the corresponding results for the case with 12 h of storage, baseload operation, and the Greenfield scenario. Rather than selecting the storage capacity that minimizes the LCOE of each technology, the capacity is fixed within each table, since the LCOE is not the sole optimization criterion of this study and the night capacity factor is an equally relevant objective. This allows the comparison to focus on how the plant design differs between technologies in terms of component sizing, PV–CSP distribution and the direction in which the optimization drives each concept. The two cases illustrate different economic drivers: at 6 h the fixed cost of the power block carries a larger weight, as it is distributed over a smaller annual

Table 5
Parameters of the 6-h optimized configurations (Night-Real strategy, Brownfield scenario).

Technology	Trough hybrid	Tower hybrid	Tower	PV BESS	Carnot
Storage capacity (h)	6	6	6	6	6
TES capacity (MWh_{th})	3700	3700	3700	–	3700
BESS capacity (MWh_{el})	–	–	–	1505	–
CSP field aperture (km^2)	0.24	0.33	1.0	–	–
CSP field nominal output (MW_{th})	166	200	550	–	–
PV field module area (km^2)	1.7	1.9	–	1.9	2.6
PV field nominal output (MW_{ac})	250	275	–	275	375
EH nominal power (MW_{el})	260	250	–	–	350
PB net nominal output (MW_{el})	250.9	250.9	250.9	–	250.9
Total land area (km^2)	5.8	6.9	5.9	5.4	8.4
Total CAPEX (M$)	451	504	436	728	491
Specific CAPEX ($/$kW_{el}$)	1799	2007	1737	2902	1956
LCOE ($/kWh)	0.1162	0.1033	0.1125	0.1579	0.0995
Night capacity factor	0.302	0.378	0.328	0.423	0.379

Table 6
Parameters of the 12-h optimized configurations (baseload strategy, Greenfield scenario).

Technology	Trough hybrid	Tower hybrid	Tower	PV BESS	Carnot
Storage capacity (h)	12	12	12	12	12
TES capacity (MWh_{th})	7400	7400	7400	–	7400
BESS capacity (MWh_{el})	–	–	–	3011	–
CSP field aperture (km^2)	0.41	0.51	3.85	–	–
CSP field nominal output (MW_{th})	277	300	2000	–	–
PV field module area (km^2)	4.8	4.6	–	4.8	6.0
PV field nominal output (MW_{ac})	700	675	–	700	875
EH nominal power (MW_{el})	450	425	–	–	600
PB net nominal output (MW_{el})	250.9	250.9	250.9	–	250.9
Total land area (km^2)	15.3	15.8	29.9	13.8	18.2
Total CAPEX (M$)	1192	1211	1464	1547	1234
Specific CAPEX ($/$kW_{el}$)	4750	4826	5835	6166	4918
LCOE ($/kWh)	0.0671	0.0653	0.0961	0.0935	0.0649
Night capacity factor	0.544	0.567	0.560	0.676	0.583

electricity production, whereas at 12 h the specific storage costs become dominant. The nominal thermal power of the CSP field refers to design point conditions, defined as a DNI of 900 W/m^2 at normal incidence.

The optimized configurations show clear design trends across the technologies. The aperture area of the CSP fields in the hybrid systems (Trough Hybrid, Tower Hybrid) is significantly smaller than in the standalone Tower, as part of the thermal input is provided by the electric heater. In contrast, the heliostat field of the standalone Tower plant is much larger, particularly in the 12-h storage configuration, where the greater receiver height and heliostat spacing increase land requirements.

The PV field area is similar for all systems, typically between 4.5 and 5 km^2 for the 12-h Greenfield designs, except for the Carnot battery, which requires a somewhat larger PV field. This is explained by the fact that PV electricity is its only source of energy, and the overall round-trip efficiency of the power-to-heat-to-power process is lower than that of direct battery storage. In both design cases, the Carnot battery also occupies a larger total land area than the hybrid systems.

In the Night-Real strategy, the nominal power of the EH is comparable to the nominal power of the PV field, since the entire PV generation is used for charging the thermal storage during daytime. In baseload operation, however, the EH capacity approximately adds up to the PB nominal output, as part of the PV electricity is exported directly to the grid while the remainder is used to charge the storage.

For the Trough Hybrid configuration, the parametric optimization leading to the lowest LCOE for each storage capacity tends to favor an oversized PV field, particularly for smaller storage capacities, in order to maximize the use of low-cost PV electricity. At the same time, the electric heater is slightly undersized, allowing a portion of PV electricity to be fed directly into the grid instead of fully converted to thermal energy.

A comparative analysis of the tables highlights two distinct economic drivers. In the 6-h Brownfield scenario, thermal-based systems benefit significantly from the reuse of existing infrastructure, achieving a specific CAPEX below 2000 $/$kW_{el}$, a benefit that does not apply to PV BESS. Conversely, the 12-h Greenfield results expose the scalability limitations of battery storage. Even when all technologies account for full power block costs, the specific CAPEX of PV BESS surges to 6166 $/$kW_{el}$ due to the linear cost increase associated with long-duration electrochemical storage. Thermal configurations, in contrast, maintain a moderate capital intensity owing to the low marginal cost of adding TES capacity. Finally, since specific CAPEX is strictly a power-based metric that ignores the capacity factor, these figures must be interpreted alongside the LCOE to accurately assess the true economic performance of each configuration.

4.4. Sensitivity analysis

A sensitivity analysis was performed by varying the costs of the BESS and CSP components, which are the two technologies whose current cost assumptions carry the greatest uncertainty. The BESS specific costs (per unit of energy capacity and power) were varied due to the cost reductions observed in recent years [44], in order to assess the impact of this trend on the results and on the storage capacity at which lower LCOEs than those of systems with TES could be achieved. For CSP, up-to-date figures are not available due to the limited deployment of new plants in recent years. CSP specific costs (parabolic troughs, receiver, heliostats, and tower) were therefore also varied to evaluate the potential impact of cost reductions driven by mass production, also considering learning curve effects reported for CSP plants in China [45]. A 30% reduction in the specific costs of all these components considered in the sensitivity analysis is shown in Table 7. The variation is not intended to represent a cost reduction potential common to all systems considered, but to account for the uncertainty of the present cost

Table 7
Cost assumptions for the sensitivity analysis.

Technology	Component	Value 2021	Unit
PT	Solar field (reference)	202	$/$m^2$
	Solar field (sensitivity analysis)	141.4	$/$m^2$
ST	Heliostat field (reference)	127	$/$m^2$
	Heliostat field (sensitivity analysis)	88.9	$/$m^2$
	Tower (reference)	88,000	$/m
	Tower (sensitivity analysis)	61,600	$/m
	Receiver (reference)	122	$/$kW_{th}$
	Receiver (sensitivity analysis)	85.4	$/$kW_{th}$
BESS	Cost per power (reference)	245	$/$kW_{el}$
	Cost per power (sensitivity analysis)	171.5	$/$kW_{el}$
	Cost per energy capacity (reference)	246	$/$kWh_{el}$
	Cost per energy capacity (sensitivity analysis)	172.2	$/$kWh_{el}$

assumptions for these two technologies. The analysis was carried out for two scenarios: the greenfield baseload configuration and the brownfield configuration under Night-Real operation.

The first scenario considered is a greenfield baseload configuration. It should be noted that this is not the most favorable scenario for CSP technology, as it particularly benefits from low-cost PV generation during daytime hours and does not take advantage of savings associated with the power block. The results are shown in Fig. 14.

The analysis shows that the PV BESS system benefits significantly from the reduction in storage costs. The LCOE crossover point with systems incorporating TES no longer occurs at around 4 h of storage, but rather at approximately 9 h of storage. The LCOE curve of the PV BESS system continues to show an increasing trend with higher storage capacity because BESS remains more expensive compared to TES; however, the slope of the curve is reduced compared to the previous specific cost assumptions.

It is also observed that reducing the cost of CSP components does not result in a proportional reduction in the LCOE of hybrid systems (Tower Hybrid and Trough Hybrid) under a baseload strategy, since reductions in the costs of the remaining components (PB, EH, and TES) are also required.

Nevertheless, a change in system design does occur, as shown in Table 8 for the 12-h optimized systems. This storage capacity was selected for the design parameters shown in both cases of the sensitivity analysis, because the larger component sizes make the effects of the cost variation more clearly visible. In this first sensitivity case, the reduced CSP costs make heat production in the Tower Hybrid system cheaper using the CSP field than with the PV + EH combination. As a result, the size of the CSP field for this technology more than doubles for large storage capacities. This effect is not observed for small storage capacities because, under this baseload strategy, the PV field is sized large to take advantage of low-cost daytime generation, and excess energy is optimized for nighttime generation without the need to increase the CSP field for lower storage capacities.

In the case of the parabolic trough hybrid system, this behavior is not observed under the baseload strategy analyzed here. The CSP field resulting from the optimization does not increase, as it is coupled to the PV field through the electric heater. Larger CSP fields do not provide additional benefits without a corresponding increase in the PV field, which does not occur because the additional storage-charging capacity would not compensate for the increased energy curtailment associated with larger system sizes.

The Carnot system does not exhibit any variation, as it does not incorporate either CSP or BESS components. It can be observed that the reduction in CSP costs causes the Carnot system to no longer be slightly cheaper than the Tower Hybrid system, instead presenting a slightly higher LCOE.

The tower system benefits the most from the reduction in CSP costs, as it is the only component responsible for heat generation in this configuration, resulting in a significantly larger percentage reduction in CAPEX. However, it still remains far from being competitive with hybrid systems.

Table 8
Sensitivity analysis: Parameters of the 12-h optimized configurations (baseload strategy, Greenfield scenario).

Technology (sensitivity analysis)	Trough hybrid	Tower hybrid	Tower	PV BESS	Carnot
Storage capacity (h)	12	12	12	12	12
TES capacity (MWh_{th})	7400	7400	7400	–	7400
BESS capacity (MWh_{el})	–	–	–	3011	–
CSP field aperture (km^2)	0.41	1.31	3.74	–	–
CSP field nominal output (MW_{th})	277	700	1950	–	–
PV field module area (km^2)	4.8	3.1	–	4.6	6.0
PV field nominal output (MW_{ac})	700	450	–	675	875
EH nominal power (MW_{el})	450	200	–	–	600
PB net nominal output (MW_{el})	250.9	250.9	250.9	–	250.9
Total land area (km^2)	15.3	16.9	28.6	13.3	18.2
LCOE ($/kWh)	0.0654	0.0615	0.0781	0.0719	0.0649
Night capacity factor	0.546	0.569	0.544	0.656	0.583

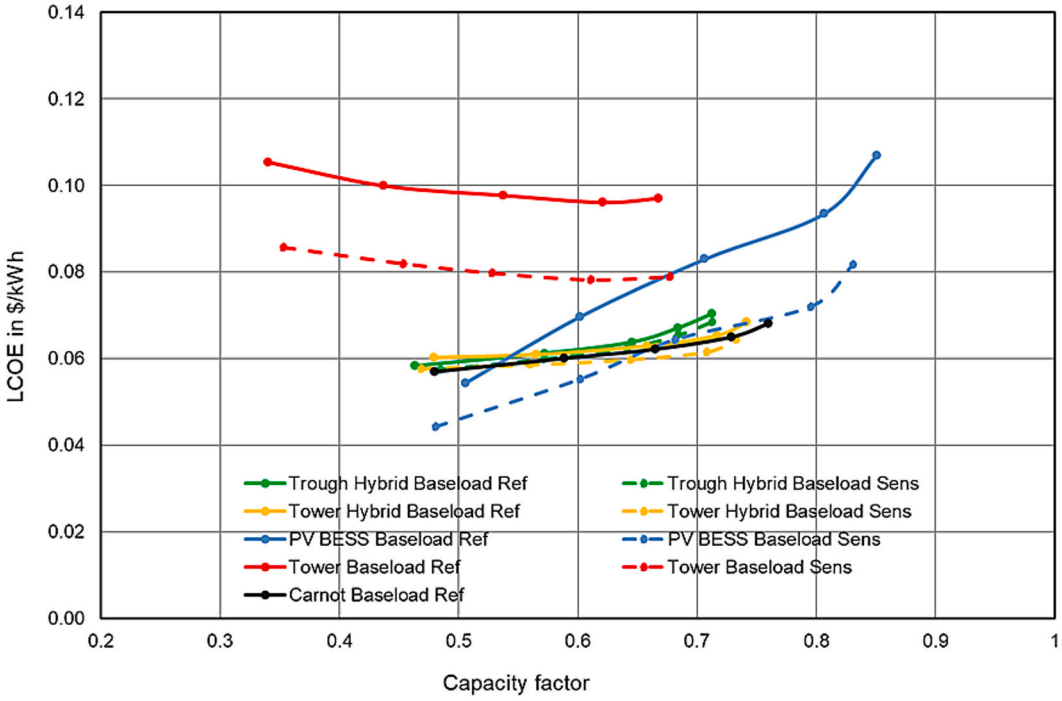


Fig. 14. Sensitivity analysis: LCOE versus capacity factor for different technologies and baseload strategy (Greenfield scenario).

It can therefore be concluded that a reduction in CSP costs alone, although it increases the CSP field size in the Tower Hybrid system, does not lead to a proportional reduction in the LCOE of the hybrid systems under a greenfield baseload strategy, since reductions in the specific costs of the remaining components (PB, EH, and TES) are also required. Under storage-based strategies and in the brownfield scenario, the LCOE advantage would be expected to be greater.

A second sensitivity analysis was therefore carried out for the brownfield configuration under Night-Real operation, using the same cost assumptions given in Table 7. The results are shown in Fig. 15, where the nighttime capacity factor is used on the x-axis, as electricity is generated exclusively at night in this operating strategy. The picture for CSP changes considerably in this second scenario compared with the first, the tower technology being clearly favored by the cost reduction. This stronger effect is mainly attributable to the brownfield assumption: since the existing power block is reused, no investment in a new PB is required, and the reduction in CSP-specific costs therefore translates into a much larger relative reduction in total plant CAPEX than in the greenfield case. For the PV BESS system, the lower storage costs lead to a substantial decrease in LCOE, but in this scenario its curve does not intersect those of the remaining systems. For the Trough Hybrid system, the reduction is again only partial, since the cost of the PV technology to which it is coupled in booster mode does not decrease, so that only part of the heat and power generation components becomes cheaper. The Carnot battery is unaffected, as none of its components is subject to the cost variations considered. The change is however significant for the tower-based systems. The standalone Tower shows a remarkable reduction in LCOE and becomes one of the least-cost systems as a result of the lower CSP costs. It is closely matched by the Tower Hybrid system which, as heat generation with CSP becomes cheaper than with PV combined with an electric heater, evolves into an essentially CSP-based configuration. This is the opposite outcome of the optimization compared with the reference cost assumptions, where the Tower Hybrid optimization tended towards a Carnot battery.

Table 9 shows the parameters defining the plant designs for a storage capacity of 12 h. The Tower Hybrid system features a considerably larger CSP field than PV field, and its design tends towards a standalone tower rather than towards a Carnot battery, as heat generation with the tower becomes cheaper. A small PV field of 100 MW_{ac} is nevertheless retained to compensate for seasonal variations and to cover parasitic consumption. The Trough Hybrid system falls behind in this scenario, with LCOE values around 20% higher than those of the tower-based systems. The PV BESS system shows the highest LCOE and the highest night capacity factor, while maintaining a comparatively low land requirement.

Table 9
Sensitivity analysis: Parameters of the 12-h optimized configurations (Night-Real strategy, Brownfield scenario).

Technology (sensitivity analysis)	Trough hybrid	Tower hybrid	Tower	PV BESS	Carnot
Storage capacity (h)	12	12	12	12	12
TES capacity (MWh_{th})	7400	7400	7400	–	7400
BESS capacity (MWh_{el})	–	–	–	3011	–
CSP field aperture (km^2)	0.53	1.71	2.13	–	–
CSP field nominal output (MW_{th})	360	900	1100	–	–
PV field module area (km^2)	3.4	0.7	–	4.3	4.7
PV field nominal output (MW_{ac})	500	100	–	625	687
EH nominal power (MW_{el})	480	100	–	–	700
PB net nominal output (MW_{el})	250.9	250.9	250.9	–	250.9
Total land area (km^2)	11.8	14.2	17.7	12.3	13.5
LCOE ($/kWh)	0.1019	0.0843	0.0853	0.1211	0.0936
Night capacity factor	0.605	0.639	0.647	0.843	0.707

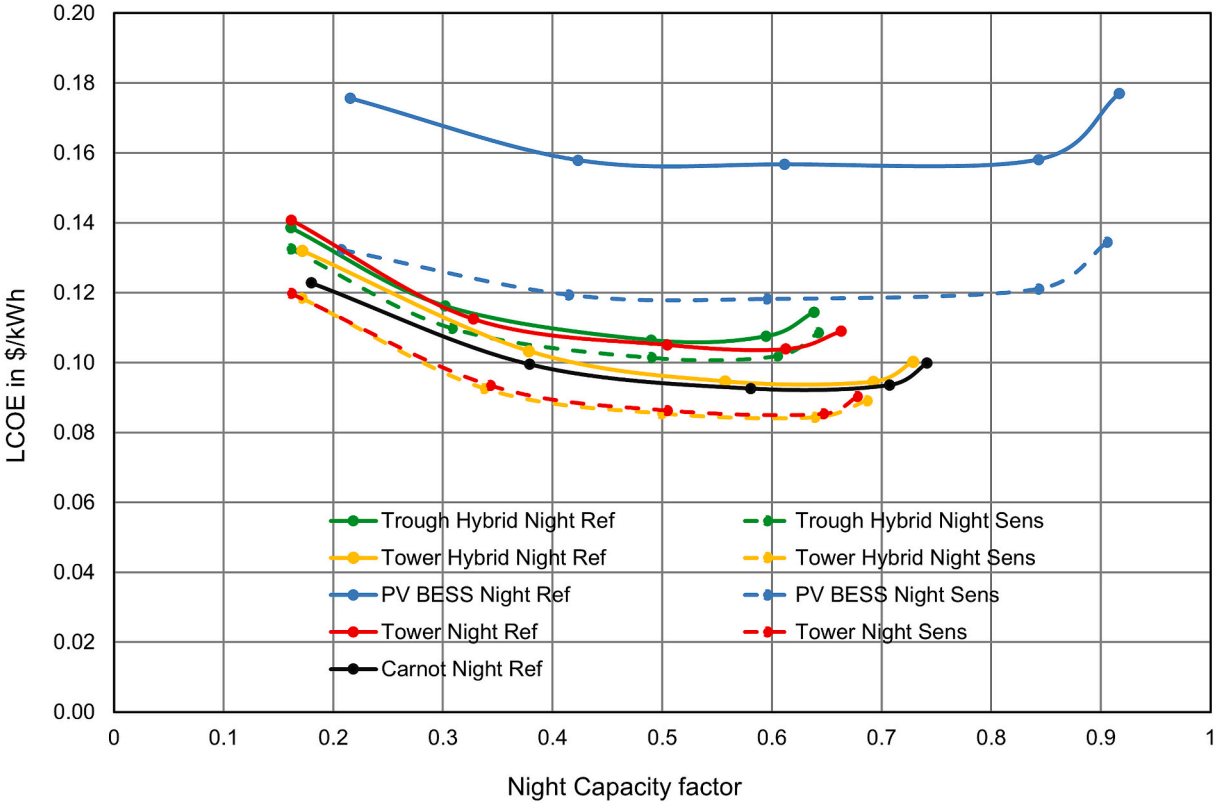


Fig. 15. Sensitivity analysis: LCOE versus night capacity factor for different technologies and Night-Real strategy (Brownfield scenario).

5. Conclusions

The conversion of the Angamos coal-fired power plant into various renewable energy concepts with solar generation and storage has been analyzed. Five energy system configurations were compared techno-economically, considering different operating strategies, storage capacities, and scenarios for power block reuse. The objective was not only to identify configurations with the lowest LCOE, but also those capable of providing the highest amount of solar electricity during nighttime, thereby supporting decarbonization and grid flexibility.

The results show very similar LCOE values for hybrid CSP-PV systems and Carnot battery systems, for baseload and storage-based (Night-Real and Night-Fict) operation strategies. The cost of heat generation using a combination of PV and an electric heater (as applied in the Carnot battery and the Tower Hybrid) is comparable, and only slightly lower, to that of a CSP field under the assumed cost parameters. Hybrid CSP-PV systems exhibit lower LCOE than a standalone CSP tower system for the baseload strategy, but similar values for nighttime-only production. Results are also highly dependent on cost assumptions and site characteristics. Slight variations in assumed costs can significantly change the comparative results.

The PV BESS system exhibits higher LCOE than hybrid CSP-PV and Carnot battery systems in a brownfield scenario for all operating strategies, as it is the only system that does not benefit from reusing the Angamos power block. This changes under the greenfield scenario with a new power block. In this case, the cost differences between systems are reduced, and the PV BESS system becomes more cost-effective for storage capacities below 4–5 h. However, costs increase with higher storage capacities due to the higher cost of batteries compared to thermal storage. In all scenarios, PV BESS demonstrates larger capacity factors than the other systems.

It should be noted that the objective of this study is not solely to minimize LCOE but also to maximize nighttime electricity production. A nighttime-focused operating strategy increases costs but also enhances nighttime generation for all systems. The chosen operating strategy is therefore a critical factor, depending on the operator's objectives.

Future cost developments will determine how the economic crossover point between technologies evolves. At present, there is significant uncertainty regarding CSP plant costs due to the limited deployment of new plants in recent years. However, as shown by the sensitivity analysis, the effect of CSP cost reductions depends strongly on the operating strategy. Under baseload operation in the greenfield scenario, reductions in CSP investment costs must be accompanied by cost reductions in the remaining components (PB, EH, and TES) in order to achieve a meaningful decrease in LCOE. Under storage-based nighttime operation in the brownfield scenario, by contrast, a reduction in CSP costs alone is sufficient for the Tower and Tower Hybrid configurations to achieve the lowest LCOE of all concepts. In the case of the PV BESS system, reductions in BESS costs do lead to a substantial decrease in LCOE, shifting the crossover point with systems incorporating TES to as much as 9 h of storage under greenfield baseload operation, although no crossover occurs in the brownfield scenario under nighttime operation. In addition, BESS costs are expected to continue declining in the future, which would further strengthen the competitiveness of PV BESS configurations.

Summarizing the results of the brownfield and greenfield scenarios, the findings clearly demonstrate the significant economic advantage of retrofitting existing power blocks in thermal power plants. Reusing the existing steam cycle substantially reduces the capital expenditure of all concepts that rely on a power block, thereby shifting the competitiveness in favor of hybrid CSP-PV systems and Carnot battery configurations. Depending on the operating strategy and the achieved capacity factor, the reuse of the existing power block lowers the LCOE by approximately 20% for baseload operation with 15 h of storage to 45% for storage-based nighttime operation with 3 h of storage, compared to equivalent greenfield installations. The strongest relative benefit is observed under storage-based nighttime operation, where the fixed costs of the power block weigh more heavily on limited annual operating hours. Overall, the results show that converting existing coal-fired power plants into hybrid solar plants or Carnot battery systems represents a technically and economically viable option that can accelerate decarbonization and increase the dispatchability of renewable generation while preserving valuable existing infrastructure.

Abbreviations

Baseload	Baseload operation with real PV
BESS	Battery Energy Storage System
CAPEX	Capital expenditure
CF	Capacity Factor
CSP	Concentrated Solar Power
DNI	Direct Normal Irradiance
EPC	Engineering, Procurement and Construction
EH	Electric Heater
GHI	Global Horizontal Irradiance
HTF	Heat Transfer Fluid
LCOE	Levelized Cost of Electricity
Night-Fict	Storage-based operation with fictional PV, nighttime discharge
Night-Real	Storage-based operation with real PV, nighttime discharge
O&M	Operations and maintenance
ORC	Organic Rankine Cycle
P2H	Power-to-Heat
P2H2P	Power-to-Heat-to-Power
PB	Power Block
PHES	Pumped Heat Energy Storage
PT	Parabolic Trough
PV	Photovoltaic
PV	BESS Photovoltaic System with Battery Energy Storage System
sCO_2	Supercritical CO_2
SG	Steam Generator
ST	Solar Tower
TES	Thermal Energy Storage
Tower Standalone	CSP solar tower plant.
Tower Hybrid	Hybrid CSP-PV plant with solar tower and thermal energy storage, with an electric heater in parallel
Trough Hybrid	Hybrid CSP-PV plant with parabolic trough and thermal energy storage, coupled through an electric heater acting as a booster
TSPP	Thermal Storage Power Plant

CRediT authorship contribution statement

Javier Iñigo-Labairu: Writing – review & editing, Writing – original draft, Visualization, Validation, Software, Methodology, Investigation, Formal analysis, Data curation, Conceptualization. **Stefano Giuliano:** Writing – review & editing, Supervision, Conceptualization. **Robert Pitz-Paal:** Supervision.

Declaration of competing interest

The authors declare that they have no known competing financial interests or personal relationships that could have appeared to influence the work reported in this paper.

Acknowledgements

This research was supported by the German Aerospace Center (DLR) through the project The Global Coal Atlas. The authors would like to thank AES Andes for the valuable technical input and support.

Data availability

Data will be made available on request.

References

[1] IRENA, Renewable Power Generation Costs in 2023, International Renewable Energy Agency, Abu Dhabi, 2024.
[2] W. Cole, V. Ramasamy, M. Turan, Cost Projections for Utility-scale Battery Storage: 2025 Update, National Renewable Energy Laboratory, Golden, CO, 2025. NREL/TP-6A40-93281, https://www.osti.gov/servlets/purl/2583471.
[3] BloombergNEF, Lithium-ion Battery Pack Prices Fall to $108 Per Kilowatt-Hour, Despite Rising Metal Prices, BloombergNEF, 2025. https://about.bnef.com/insights/clean-transport/lithium-ion-battery-pack-prices-fall-to-108-per-kilowatt-hour-despite-rising-metal-prices-bloombergnef/ (accessed 1 February 2026).
[4] REN21, Global Status Report 2025: Renewables in Energy Supply – Concentrated Solar Thermal Power (CSP) Factsheet. REN21. https://www.ren21.net/gsr-2025/technologies/csp/, 2025.
[5] International Energy Agency, Coal in Net Zero Transitions: Executive Summary, International Energy Agency, Paris, 2024. https://www.iea.org/reports/coal-in-net-zero-transitions/executive-summary.
[6] International Energy Agency, World Energy Outlook 2023, OECD/IEA, 2023. https://www.iea.org/reports/world-energy-outlook-2023.
[7] Global Energy Monitor, Boom and Bust Coal 2025: Tracking the Global Coal Plant Pipeline. https://globalenergymonitor.org/wp-content/uploads/2025/03/Boom-Bust-Coal-2025.pdf, 2025.
[8] Global Energy Monitor, Estimating Carbon Dioxide Emissions from Coal Plants. https://www.gem.wiki/Estimating_carbon_dioxide_emissions_from_coal_plants, 2025.
[9] Global Energy Monitor, Global Coal Plant Tracker, 2025. https://globalenergymonitor.org/projects/global-coal-plant-tracker/.
[10] K.M. Powell, K. Rashid, K. Ellingwood, J. Tuttle, B.D. Iverson, Hybrid concentrated solar thermal power systems: a review, Renew. Sust. Energ. Rev. 80 (2017) 215–237, https://doi.org/10.1016/j.rser.2017.05.067.
[11] X. Ju, C. Xu, Y. Hu, X. Han, G. Wei, X. Du, A review on the development of photovoltaic/concentrated solar power (PV-CSP) hybrid systems, Sol. Energy Mater. Sol. Cells 161 (2017) 305–327, https://doi.org/10.1016/j.solmat.2016.12.004.
[12] B.A.A. Yousef, A.A. Hachicha, I. Rodriguez, M.A. Abdelkareem, A. Inyaat, Perspective on integration of concentrated solar power plants, Int. J. Low-Carbon Technol. 16 (3) (2021) 1098–1125, https://doi.org/10.1093/ijlct/ctab034.
[13] J. Iñigo-Labairu, J. Dersch, L. Schomaker, Integration of CSP and PV power plants: investigations about synergies by close coupling, Energies 15 (2022) 7103, https://doi.org/10.3390/en15197103.
[14] J. Iñigo-Labairu, J. Dersch, T. Hirsch, S. Giuliano, M. Loevenich, D.A. Cordoba Lopez, Techno-economic evaluation of CSP–PV hybrid plants with heat pump in a temperature booster configuration, Energies 17 (2024) 2634, https://doi.org/10.3390/en17112634.
[15] S. Guccione, R. Guedez, Techno-economic optimization of molten salt based CSP plants through integration of supercritical CO_2 cycles and hybridization with PV and electric heaters, Energy 283 (2023) 128528, https://doi.org/10.1016/j.energy.2023.128528.
[16] C. Parrado, A. Girard, F. Simon, E. Fuentealba, 2050 LCOE projection for a hybrid PV-CSP plant in the Atacama Desert, Chile, Energy 94 (2016) 422–430, https://doi.org/10.1016/j.energy.2015.11.015.
[17] A.R. Starke, J.M. Cardemil, R.A. Escobar, S. Colle, Assessing the performance of hybrid CSP + PV plants in northern Chile, Sol. Energy 138 (2016) 88–97, https://doi.org/10.1016/j.solener.2016.09.006.
[18] A. Zurita, C.E. Mata-Torres, C. Valenzuela, C. Felbol, J.M. Cardemil, A.M. Guzmán, R.A. Escobar, Techno-economic evaluation of a hybrid CSP + PV plant integrated with thermal energy storage and a large-scale battery energy storage system for base generation, Sol. Energy 173 (2018) 1262–1277, https://doi.org/10.1016/j.solener.2018.08.061.
[19] O. Behar, D. Sbarbaro, L. Moran, Which is the most competitive solar power technology for integration into the existing copper mining plants: photovoltaic (PV), Concentrating Solar Power (CSP), or hybrid PV-CSP? J. Clean. Prod. 287 (2021) 125455 https://doi.org/10.1016/j.jclepro.2020.125455.
[20] J.A. Aguilar-Jiménez, N. Velázquez, A. Acuña, R. Cota, E. González, L. González, R. López, S. Islas, Techno-economic analysis of a hybrid PV-CSP system with thermal energy storage applied to isolated microgrids, Sol. Energy 174 (2018) 55–65, https://doi.org/10.1016/j.solener.2018.08.078.
[21] L. Pilotti, M. Colombari, A.F. Castelli, M. Binotti, A. Giaconia, E. Martelli, Simultaneous design and operational optimization of hybrid CSP-PV plants, Appl. Energy 331 (2023) 120369, https://doi.org/10.1016/j.apenergy.2022.120369.
[22] G. Furlan, F. You, Robust design of hybrid solar power systems: sustainable integration of concentrated solar power and photovoltaic technologies, Adv. Appl. Energy 13 (2024) 100164, https://doi.org/10.1016/j.adapen.2024.100164.
[23] A. Zurita, C.E. Mata-Torres, J.M. Cardemil, R. Guédez, R.A. Escobar, Multi-objective optimal design of solar power plants with storage systems according to dispatch strategy, Energy 237 (2021) 121627, https://doi.org/10.1016/j.energy.2021.121627.
[24] M. Geyer, S. Giuliano, Conversion of existing coal plants into thermal storage plants, Encyclopedia of Energy Storage 2 (2022) 122–132, https://doi.org/10.1016/B978-0-12-819723-3.00117-7.
[25] O. Dumont, G.F. Frate, A. Pillai, S. Lecompte, M. De Paepe, V. Lemort, Carnot battery technology: a state-of-the-art review, J. Energy Storage 32 (2020) 101756, https://doi.org/10.1016/j.est.2020.101756.
[26] G.F. Frate, L. Ferrari, U. Desideri, Rankine Carnot batteries with the integration of thermal energy sources: a review, Energies 13 (18) (2020) 4766, https://doi.org/10.3390/en13184766.
[27] V. Novotny, V. Basta, P. Smola, J. Spale, Review of Carnot battery technology commercial development, Energies 15 (2) (2022) 647, https://doi.org/10.3390/en15020647.
[28] T. Liang, A. Vecchi, K. Knobloch, A. Sciacovelli, K. Engelbrecht, Y. Li, Y. Ding, Key components for Carnot batteries: technology review, technical barriers and selection criteria, Renew. Sust. Energ. Rev. 161 (2022) 112478, https://doi.org/10.1016/j.rser.2022.112478.
[29] A. Vecchi, K. Knobloch, T. Liang, H. Kildahl, A. Sciacovelli, K. Engelbrecht, Y. Li, Y. Ding, Carnot batteries (CB): a state-of-the-art review of CB system performance and applications, J. Energy Storage 49 (2022) 105782, https://doi.org/10.1016/j.est.2022.105782.
[30] W. Arnold, S. Giuliano, G. Koll, M. May, T. Bauer, S. Belik, S. Bohnes, J. Dersch, V. Dreißigacker, M.P. Geyer, N. Handschuh, U. Herrmann, F. Klasing, M. Krüger, K. Noureldin, M.I. Roldan Serrano, D. Stollenwerk, J. Schulte, F. Trieb, S. Zunft, StoreToPower - Phase 1: Stromspeicherung in Hochtemperatur-Wärmespeicherkraftwerken, Project Report (2022) 47–72. https://elib.dlr.de/186474/.
[31] M.I. Roldán Serrano, K. Knobloch, S. Giuliano, K. Engelbrecht, T. Hirsch, Retrofit of a coal-fired power plant with a rock bed thermal energy storage, J. Energy Storage 75 (2024) 109238, https://doi.org/10.1016/j.est.2023.109238.
[32] M. Geyer, S. Giuliano, F. Trieb, Repurposing of Existing Coal-fired Power Plants into Thermal Storage Plants for Renewable Power in Chile, Final Report and Executive Summary, DLR/GIZ, 2020, https://4echile.cl/publicaciones/reconversion-de-centrales-a-carbon-en-plantas-de-almacenamiento-termico-con-energia-renovable-en-chile/.
[33] B. Truong, B. Bollinger, Repurposing Fossil-fueled Assets for Energy Storage (Final Report, DE-FE0032004), 2022, https://doi.org/10.2172/1874051.
[34] Enervis, Techno-economic Assessment of Replacement Options for Ptolemaida V. https://thegreentank.gr/wp-content/uploads/2021/04/2021_CE_GT_P5_Replacement_Technologies_Report.pdf, 2021.
[35] Z. Zhang, M. Zhou, B. Yuan, Z. Wu, J. Liu, S. Liu, Z. Guo, G. Li, Decarbonizing the power system by co-planning coal-fired power plant transformation and energy storage, J. Energy Storage 66 (2023) 107442, https://doi.org/10.1016/j.est.2023.107442.
[36] Z. Zhang, M. Zhou, B. Yuan, Z. Guo, Z. Wu, G. Li, Multipath retrofit planning approach for coal-fired power plants in low-carbon power system transitions: Shanxi Province case in China, Energy 275 (2023) 127502, https://doi.org/10.1016/j.energy.2023.127502.
[37] B. Li, W. Qian, X. Du, Study on the retrofit of coupled Carnot battery in retired coal-fired power units for grid energy storage transformation, Appl. Energy 401 (2025) 126796, https://doi.org/10.1016/j.apenergy.2025.126796.
[38] F. Klasing, M. Prenzel, T. Bauer, Repurposing of supercritical coal plants into highly flexible grid storage with adapted 620°C nitrate salt technology, Appl. Energy 377 (2025) 124524, https://doi.org/10.1016/j.apenergy.2024.124524.
[39] German Aerospace Center (DLR), greenius [Software]. http://freegreenius.dlr.de, 2025.
[40] Iqony, EBSILON® Professional [Software]. https://www.ebsilon.com/de/, 2025.
[41] P. Schwarzbözl, R. Pitz-Paal, M. Schmitz, Visual HFLCAL – a software tool for layout and optimisation of heliostat fields, in: Proceedings of SolarPACES 2009, 2009.
[42] Meteotest., Meteonorm Version 8 [Software]. https://meteonorm.com, 2020.
[43] C. Prieto, L. Miró, G. Peiró, E. Oró, A. Gil, L.F. Cabeza, Temperature distribution and heat losses in molten salts tanks for CSP plants, Sol. Energy 135 (2016) 518–526, https://doi.org/10.1016/j.solener.2016.06.030.
[44] BloombergNEF, New record lows for battery prices, BloombergNEF, 2025. https://about.bnef.com/insights/clean-transport/new-record-lows-for-battery-prices/. (Accessed 1 February 2026).
[45] A. Schweitzer, T. Keck, A. Oschatz, D. Sun, X. Zhao, Cost reduction through learning curve effects at CSP power plants in China, in: Conference Presentation, SolarPACES 2025, Almería, Spain, 23–26 September 2025.